

Controlling Emission Energy, Self-Quenching, and Excimer Formation in Highly Luminescent N[∧]C[∧]N-Coordinated Platinum(II) Complexes

Sarah J. Farley, David L. Rochester, Amber L. Thompson, Judith A. K. Howard, and J. A. Gareth Williams*

Department of Chemistry, University of Durham, South Road, Durham DH1 3LE, U.K.

Received June 25, 2005

A series of cyclometalated platinum(II) complexes have been prepared, [PtL¹Cl], containing N[∧]C[∧]N-coordinating, terdentate ligands based on 1,3-dipyridylbenzene (HL¹), incorporating aryl substituents at the central 5 position of the ligand. All of the new complexes are intensely luminescent in a degassed solution at 298 K ($\phi = 0.46$ – 0.65 in CH₂Cl₂) with lifetimes in the microsecond range (7.9–20.5 μ s). The introduction of the aryl substituents leads to a red shift in the lowest-energy, intense charge-transfer absorption band compared to [PtL¹Cl] (401 nm in CH₂Cl₂), in the order H < mesityl < 2-pyridyl < 4-tolyl < 4-biphenyl < 2-thienyl < 4-(dimethylamino)phenyl (431 nm in CH₂Cl₂), which correlates with the decreasing order of oxidation potentials. A similar order is also observed in the emission maxima, ranging from 491 nm for [PtL¹Cl] to 588 nm for the 4-(dimethylamino)phenyl-substituted complex. The emission spectra of all of the complexes, except for the amino-substituted compound, are highly structured in a dilute solution in CH₂Cl₂, and the emission is assigned to excited states of primarily ³LC (ligand-centered) character. At higher concentrations, self-quenching accompanied by structureless excimer emission centered at 700 nm is observed, but the aryl groups attenuate the self-quenching compared to the parent compound [PtL¹Cl], particularly for the most sterically hindered mesityl complex. The introduction of the strongly electron-donating 4-dimethylamino substituent leads to a switch in the nature of the lowest-energy excited state from ³LC to one of primarily intraligand charge-transfer (ILCT) character in CH₂Cl₂: this complex displays a structureless and much broader emission band than the other compounds and a high degree of positive solvatochromism. No excimer emission is observed in CH₂Cl₂, and self-quenching is an order of magnitude lower than that for the other complexes. However, in nonpolar solvents such as CCl₄, the ILCT state is destabilized, such that the ³LC remains the lowest-energy excited state. Reversible switching between the ILCT and ³LC states can also be achieved in a CH₂Cl₂ solution by protonation of the amine, with an accompanying large change in the emission maxima of >100 nm. The X-ray structures of the biphenyl- and methyl-substituted complexes are reported, together with those of the 2-pyridyl- and mesityl-substituted ligands and the key synthetic intermediate 1-bromo-3,5-di(2-pyridyl)benzene.

Introduction

In the field of inorganic photochemistry, the coordinative unsaturation of square-planar platinum(II) complexes gives rise to the possibility of ground- and excited-state interactions that are not possible in octahedral and tetrahedral metal complexes. Such axial interactions can lead, inter alia, to self-quenching and cross-quenching, including excimer and exciplex formation,^{1–4} to aggregation and switching between

excited states of different orbital origin according to the concentration and proximity of the molecules,^{5,6} and to chemical and photochemical reactivity.^{7,8} Potential applica-

* To whom correspondence should be addressed. E-mail: j.a.g.williams@durham.ac.uk.

(1) (a) Connick, W. B.; Gray, H. B. *J. Am. Chem. Soc.* **1997**, *119*, 11620. (b) Fleeman, W. L.; Connick, W. B. *Spectrum (Bowling Green, OH, U.S.)* **2002**, *15*, 14.

(2) Pettijohn, C. N.; Jochowitz, E. B.; Chuong, B.; Nagle, J. K.; Vogler, A. *Coord. Chem. Rev.* **1998**, *171*, 85.
(3) Connick, W. B.; Geiger, D.; Eisenberg, R. *Inorg. Chem.* **1999**, *38*, 3264.
(4) Crites Tears, D. K.; McMillin, D. R. *Coord. Chem. Rev.* **2001**, *211*, 195.
(5) For example, see: (a) Miskowski, V. M.; Houlding, V. H. *Inorg. Chem.* **1991**, *30*, 4446. (b) Field, J. S.; Haines, R. J.; McMillin, D. R.; Summerton, G. C. *J. Chem. Soc., Dalton Trans.* **2002**, 1369. (c) Yam, V. W.-W.; Wong, K. M. C.; Zhu, N. Y. *J. Am. Chem. Soc.* **2002**, *124*, 6506.
(6) Lai, S.-W.; Chan, M. C. W.; Cheung, T.-C.; Peng, S.-M.; Che, C.-M. *Inorg. Chem.* **1999**, *38*, 4046.

tions arising from such interactions include chemical sensing and vapochromism⁷ and the development of molecular probes for biological macromolecules.⁹ In addition, the triplet nature of the luminescence of platinum(II) metal complexes, promoted by the high spin-orbit coupling constant of the metal ion, renders the most emissive complexes of interest for use in optoelectronics, for example, as triplet-harvesting agents in organic light-emitting devices (OLEDs).¹⁰

Many simple platinum(II) complexes, such as [Pt-(bpy)₂Cl₂], are either nonemissive or only very weakly luminescent at room temperature, owing to the presence of low-lying metal-centered (d-d) excited states, which are severely distorted compared to the ground state and hence subject to efficient nonradiative decay.¹¹ Three distinct strategies have emerged to promote luminescence from pyridyl-based platinum(II) complexes. Che et al. have shown that the introduction of aryl substituents at the 4' position of the terpyridine ligand in [Pt(tpy)Cl]⁺ leads to emission in a fluid solution at room temperature, with lifetimes on the microsecond time scale.¹² The influence of the substituents is most pronounced for the most electron-rich groups. McMillin and co-workers have interpreted a similar effect of polycyclic aromatic substituents, such as 9-phenanthrenyl and 1-pyrenyl, in terms of a switch from the usual metal-to-ligand charge-transfer state (³MLCT) to a lower-energy state with significant aryl-to-tpy intraligand charge transfer (¹³ILCT).¹³ The ILCT state is not subject to efficient nonradiative decay via the higher-lying d-d state, and a luminescence lifetime as long as 64 μ s has been observed for the 1-pyrenyl-substituted complex.^{13b,c} The other two approaches seek to increase the ligand field strength at the metal in order to raise the energy of the deactivating d-d state and hence reduce its influence. This may be achieved through the replacement of the chloride ligands in, for example, [Pt(tpy)Cl]⁺ or [Pt(bpy)Cl₂], by a strong-field ligand such as an acetylide $\text{C}\equiv\text{CR}$, leading to complexes that are emissive at room temperature.¹⁴⁻¹⁷ Alternatively, the poly-

pyridyl ligand can be replaced by a cyclometalating analogue because the very strong ligand field induced by the cyclometalated carbon again serves to raise the energy of the deactivating d-d states. This strategy has led to a variety of emissive complexes, including several containing N \wedge C-coordinated ligands such as 2-phenylpyridine.^{8c,10a,d,18,19} A rich chemistry of platinum(II) with cyclometalating terdentate ligands has also been developed.²⁰⁻²⁴ The platinum(II) complexes of N \wedge N \wedge C-binding ligands²⁰ [e.g., 6-phenyl-2,2'-bipyridine (phbpy) and analogues] display ³MLCT emission, which has been explored in a variety of applications, particularly by Che and co-workers.^{6,10c,21} Bis-cyclometalated, C \wedge N \wedge C-coordinated platinum(II) complexes (e.g., with 2,6-diphenylpyridine) display emission from a ³LC (ligand-centered) state.²²

In the case of N \wedge C \wedge N-coordinated platinum(II) complexes, two distinct types of behavior have emerged. Connick and co-workers have observed low-energy, metal-centered emission at 77 K from complexes with cyclometalating "pincer" ligands, in which the lateral coordinating nitrogen atoms are aliphatic amines [e.g., the 2,6-bis(piperidylmethyl)-phenyl anion].²³ On the other hand, we recently discovered that the N \wedge C \wedge N coordination of platinum(II) by 1,3-dipyridylbenzene (HL¹) leads to a highly luminescent complex, [PtL¹Cl] (Chart 1), which emits from a ³LC state.²⁴ Two simple derivatives incorporating alkyl or ester substituents at the 5 position of the central benzene ring were also prepared (Chart 1), displaying small red and blue shifts of the emission, respectively, when compared to the parent

- (7) For example, see: (a) Buss, C. E.; Mann, K. R. *J. Am. Chem. Soc.* **2002**, *124*, 1031. (b) Grove, L. J.; Rennekamp, J. M.; Jude, H.; Connick, W. B. *J. Am. Chem. Soc.* **2004**, *126*, 1594. (c) Wadas, T. J.; Wang, Q. M.; Kim, Y. J.; Flaschenreim, C.; Blanton, T. N.; Eisenberg, R. *J. Am. Chem. Soc.* **2004**, *126*, 16841.
- (8) (a) Chassot, L.; von Zelewsky, A.; Sandrini, D.; Maestri, M.; Balzani, V. *J. Am. Chem. Soc.* **1986**, *108*, 6084. (b) Chassot, L.; von Zelewsky, A. *Helv. Chim. Acta* **1986**, *69*, 1855. (c) Sandrini, D.; Maestri, M.; Balzani, V.; Chassot, L.; von Zelewsky, A. *J. Am. Chem. Soc.* **1987**, *109*, 7720.
- (9) McMillin, D. R.; Moore, J. J. *Coord. Chem. Rev.* **2002**, *229*, 113.
- (10) For example, see: (a) Brooks, J.; Babayan, Y.; Lamansky, S.; Djurovich, P. I.; Tsyba, I.; Bau, R.; Thompson, M. E. *Inorg. Chem.* **2002**, *41*, 3055. (b) Cocchi, M.; Fattori, V.; Virgili, D.; Sabatini, C.; Di Marco, P.; Maestri, M.; Kalinowski, J. *Appl. Phys. Lett.* **2004**, *84*, 1052. (c) Lu, W.; Mi, B.-X.; Chan, M. C. W.; Hui, Z.; Che, C.-M.; Zhu, N.; Lee, S.-T. *J. Am. Chem. Soc.* **2004**, *126*, 4958. (d) Ionkin, A. S.; Marshall, W. J.; Wang, Y. *Organometallics* **2005**, *24*, 619.
- (11) (a) Aldridge, T. K.; Stacy, E. M.; McMillin, D. R. *Inorg. Chem.* **1994**, *33*, 722. (b) Miskowski, V. M.; Houlding, V. H.; Che, C.-M.; Wang, Y. *Inorg. Chem.* **1993**, *32*, 2518.
- (12) Yip, H.-K.; Cheng, L.-K.; Cheung, K.-K.; Che, C. M. *J. Chem. Soc., Dalton Trans.* **1993**, 2933.
- (13) (a) Crites, D. K.; Cunningham, C. T.; McMillin, D. R. *Inorg. Chim. Acta* **1998**, *273*, 346. (b) Michalec, J. F.; Bejune, S. A.; McMillin, D. R. *Inorg. Chem.* **2000**, *39*, 2708. (c) Michalec, J. F.; Bejune, S. A.; Cottell, D. G.; Summerton, G. C.; Gertenbach, J. A.; Field, J. S.; Haines, R. J.; McMillin, D. R. *Inorg. Chem.* **2001**, *40*, 2193.

- (14) (a) Hissler, M.; Connick, W. B.; Geiger, D. K.; McGarrah, J. E.; Lipa, D.; Lachicotte, R. J.; Eisenberg, R. *Inorg. Chem.* **2000**, *39*, 447. McGarrah, J. E.; Kim, Y.-J.; Hissler, M.; Eisenberg, R. *Inorg. Chem.* **2001**, *40*, 4510. McGarrah, J. E.; Eisenberg, R. *Inorg. Chem.* **2003**, *42*, 4355. (b) Hua, F.; Kinayyigit, S.; Cable, J. R.; Castellano, F. N. *Inorg. Chem.* **2005**, *44*, 471.
- (15) (a) Yam, V. W.-W.; Tang, R. P. L.; Wong, K. M. C.; Cheung, K. K. *Organometallics* **2001**, *20*, 4476. (b) Wong, K. M.-C.; Tang, W.-S.; Lu, X.-X.; Zhu, N.; Yam, V. W.-W. *Inorg. Chem.* **2005**, *44*, 1492.
- (16) (a) Yang, Q.-Z.; Wu, L.-Z.; Wu, Z.-X.; Zhang, L.-P.; Tung, C.-H. *Inorg. Chem.* **2002**, *41*, 5653. (b) Yang, Q.-Z.; Tong, Q.-X.; Wu, L.-Z.; Wu, Z.-X.; Zhang, L.-P.; Tung, C.-H. *Eur. J. Inorg. Chem.* **2004**, 1948.
- (17) (a) Whittle, C. E.; Weinstein, J. A.; George, M. W.; Schanze, K. S. *Inorg. Chem.* **2001**, *40*, 4053. (b) Haskins-Glusac, K.; Ghiviriga, I.; Abboud, K. A.; Schanze, K. S. *J. Phys. Chem. B* **2004**, *108*, 4969.
- (18) Chassot, L.; Müller, E.; von Zelewsky, A. *Inorg. Chem.* **1984**, *23*, 4249. Maestri, M.; Sandrini, D.; Balzani, V.; Chassot, L.; Jolliet, P.; von Zelewsky, A. *Chem. Phys. Lett.* **1985**, *122*, 375.
- (19) (a) Craig, C. A.; Garces, F. O.; Watts, R. J.; Palmans, R.; Frank, A. *J. Coord. Chem. Rev.* **1990**, *97*, 193. Mdeleeni, M. M.; Bridgewater, J. S.; Watts, R. J.; Ford, P. C. *Inorg. Chem.* **1995**, *34*, 2334. (b) Kvam, P.-I.; Puzyk, M. V.; Balashev, K. P.; Songstad, J. *Acta Chem. Scand.* **1995**, *49*, 335. Balashev, K. P.; Puzyk, M. V.; Kotlyar, V. S.; Kulikova, M. V. *Coord. Chem. Rev.* **1997**, *159*, 109.
- (20) Constable, E. C.; Henney, R. P. G.; Leese, T. A.; Tocher, D. A. *J. Chem. Soc., Chem. Commun.* **1990**, 513.
- (21) For example, see: (a) Lu, W.; Zhu, N.; Che, C.-M. *Chem. Commun.* **2002**, 900. (b) Che, C.-M.; Zhang, J.-L.; Lin, L.-R. *Chem. Commun.* **2002**, 2556. (c) Che, C.-M.; Fu, W.-F.; Lai, S.-W.; Hou, Y.-J.; Liu, Y.-L. *Chem. Commun.* **2003**, 118.
- (22) Yam, V. W.-W.; Tang, R. P.-L.; Wong, K. M.-C.; Lu, X.-X.; Cheung, K.-K.; Zhu, N. *Chem.—Eur. J.* **2002**, *8*, 4066.
- (23) Jude, H.; Kraus Bauer, J. A.; Connick, W. B. *Inorg. Chem.* **2002**, *41*, 2275. Replacement of the halide ligand in such complexes by, for example, 4-phenylpyridine results in a switch to pyridyl ligand-centered ³ π - π^* emission: Jude, H.; Kraus Bauer, J. A.; Connick, W. B. *Inorg. Chem.* **2004**, *43*, 725.
- (24) Williams, J. A. G.; Beeby, A.; Davies, E. S.; Weinstein, J. A.; Wilson, C. *Inorg. Chem.* **2003**, *42*, 8609.

Scheme 1

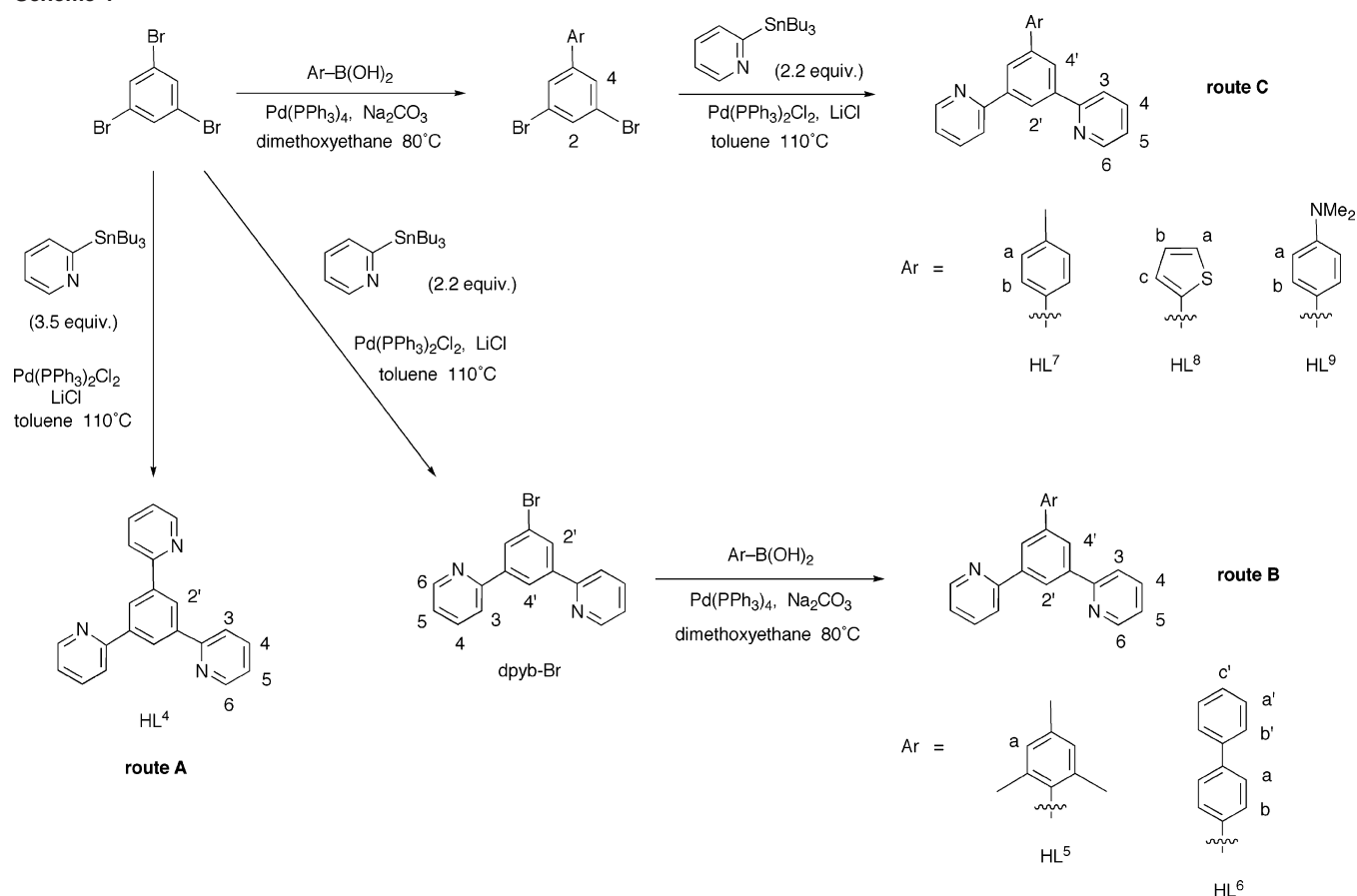
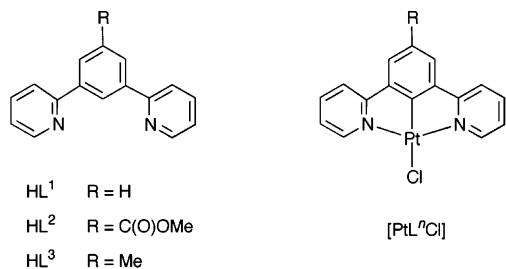


Chart 1



complex. The luminescence quantum yields of 0.58–0.68 and lifetimes of 7.0–8.0 μs (in degassed CH_2Cl_2) are an order of magnitude greater than those for analogous $\text{Pt(N}^{\wedge}\text{N}^{\wedge}\text{C)-Cl}$ complexes, attributed to the very short Pt–C bond in the $\text{N}^{\wedge}\text{C}^{\wedge}\text{N}$ -coordinated complexes.²⁴ This serves to further raise the energy of the d–d excited state, effectively severing completely this pathway of nonradiative deactivation.

In this paper, we describe the synthesis and luminescence properties of a new series of $\text{N}^{\wedge}\text{C}^{\wedge}\text{N}$ -coordinated complexes incorporating pendent aryl groups at the 5 position and demonstrate that the introduction of such substituents not only enables the excited-state energy to be varied over a wide range of at least 5000 cm^{-1} , while maintaining the exceptionally high quantum yields, but also allows the rate of self-quenching and extent of excimer formation to be controlled. The unique luminescence properties of a *p*-(dimethylamino)-phenyl-substituted complex, which are profoundly modified upon protonation of the amine, are also described.

Results and Discussion

Synthesis and Characterization of Ligands. The 5-aryl-substituted 1,3-dipyridylbenzene ligands were prepared from 1,3,5-tribromobenzene (tbb) using different sequences of cross-coupling reactions, as shown in Scheme 1. The C_3 -symmetric ligand 1,3,5-tris(2-pyridyl)benzene, HL^4 , was prepared readily in one step by palladium-catalyzed Stille cross-coupling of tbb with an excess of 2-(tri-*n*-butylstannyl)pyridine in toluene (Scheme 1, route A). All of the other ligands have 2-fold symmetry, and their syntheses require the selective substitution of two of the three bromine atoms of tbb with pyridyl moieties and the third bromine atom with the appropriate aryl group. Previous syntheses of 5-aryl-1,3-dipyridylbenzenes have proceeded via the intermediate 1-bromo-3,5-di(2-pyridyl)benzene (dpyb-Br), obtained by cross-coupling of tbb with 2 equiv of (trialkylstannyl)pyridine^{25a} or with a related organozinc species prepared in situ (Negishi-type coupling);^{25b,c} the remaining bromine atom is then available for further cross-coupling to introduce the requisite aryl group. This route was employed here to prepare the mesityl- and biphenyl-substituted ligands HL^5 and HL^6 by reaction of dpyb-Br with mesitylboronic acid and 4-biphenylboronic acid, respectively, in a Suzuki-type cross-coupling (Scheme 1, route B). Previous work on the synthesis

(25) (a) Beley, M.; Chodorowski, S.; Collin, J.-P.; Sauvage, J.-P. *Tetrahedron Lett.* **1993**, 34, 2933. (b) Jouaiti, A.; Geoffroy, M.; Collin, J.-P. *Inorg. Chim. Acta* **1996**, 245, 69. (c) Chavarot, M.; Pikramenou, Z. *Tetrahedron Lett.* **1999**, 40, 6865.

of dpyb-Br by Stille coupling reported yields of 35%.^{25a} It was noted during the present work that this compound is susceptible to competitive hydro-debromination under the Stille conditions. Thus, the proportion of the desired product in the reaction mixture initially increases as the Stille coupling proceeds but then begins to fall off as debromination occurs to give HL¹. The optimal reaction time was found to be about 20–24 h, leading to yields of 50–55%. Significant quantities of HL¹ side product were isolated when longer reaction times were employed.

An alternative approach of monosubstituting the tbb starting material with the requisite aryl group by Suzuki coupling, prior to reaction with the stannylpyridine, was also investigated and shown to be a viable alternative. Ligands HL⁷, HL⁸, and HL⁹ were prepared in this way (Scheme 1, route C): palladium-catalyzed Suzuki cross-coupling of tbb with the appropriate arylboronic acid, and chromatographic purification to remove disubstituted material and unreacted tbb, was followed by Stille coupling with 2-(tri-*n*-butylstannyl)pyridine.

The ligands were characterized by two-dimensional ¹H and ¹³C NMR spectroscopy, mass spectrometry, and elemental analysis. Complete assignment of ¹H NMR spectra was possible using ¹H–¹H NOESY spectroscopy, which crucially allows resonances on the pendent ring to be assigned on the basis of the through-space coupling of H^b to H^{4'} (for ligands HL⁶–HL⁹; the atom-numbering system is shown in Scheme 1).

(a) Crystal Structures of dpyb-Br, HL⁴, and HL⁵. Single crystals of these compounds suitable for X-ray diffraction analysis were obtained by the slow evaporation of a dichloromethane solution containing the ligand. The crystal structure of dpyb-Br (Figure 1a) shows a head-to-tail disposition of the two pyridyl rings. This configuration may be adopted to minimize unfavorable electrostatic interactions between the lone pairs and resembles the *transoid* arrangement of the pyridine units about the interannular bonds in 2,2':6',2''-terpyridines.^{26,27} However, both nitrogen atoms participate in weak intermolecular C–H···N interactions, which may also influence the configuration [C···N = 3.407(3) and 3.495(3) Å for C11–H11···N1 and C14–H14···N2, respectively]. The three aromatic rings are not quite coplanar, with angles of 8.34(11)° and 26.35(8)° between the planes of the lateral pyridyl rings and that of the central benzene ring. There are no other examples of uncoordinated 1,3-di-(2-pyridyl)benzenes in the Cambridge Crystallographic Database to enable structural comparisons to be performed. However, the structure of 1,3-di(quinolin-2-yl)benzene displays a similar head-to-tail arrangement of the quinolyl groups, albeit with larger angles of 41.1 and 57.5° between the planes of the quinolyl rings and the central aryl ring.²⁸

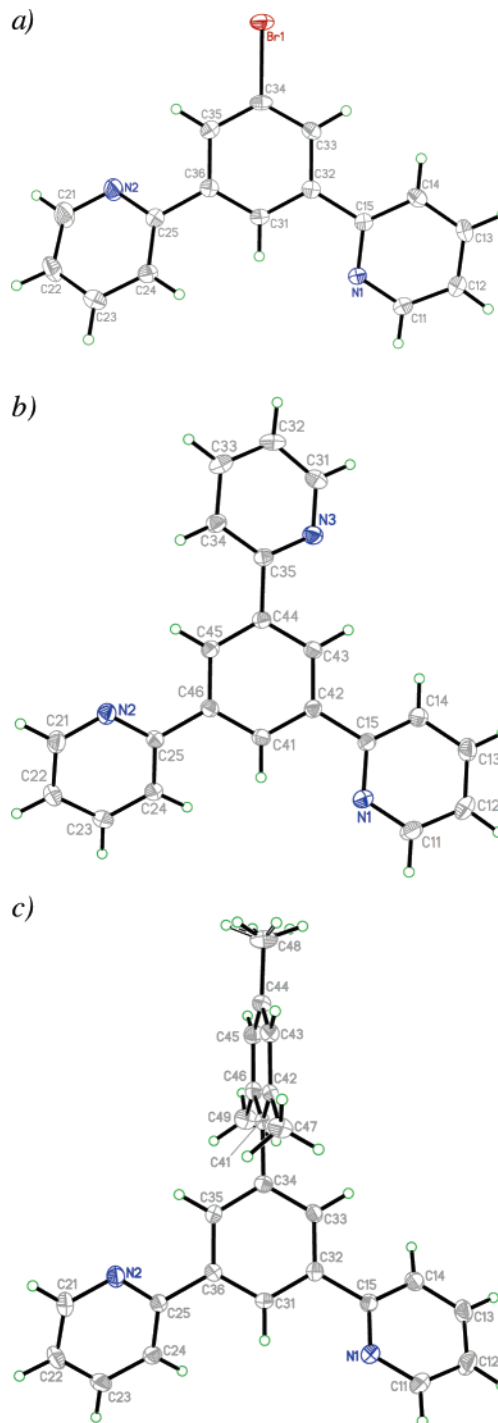


Figure 1. Molecular structures of the key synthetic intermediate dpyb-Br (a) and of ligands HL⁴ (b) and HL⁵ (c) at 120 K, with displacement ellipsoids at the 50% level.

X-ray diffraction analyses of single crystals of HL⁴ and HL⁵ reveal similar features (parts b and c of Figure 1, respectively). In the case of HL⁴, there are three pyridyl groups, and all three adopt a head-to-tail arrangement (i.e., with a pseudo C₃ axis through the center of the benzene ring). The pyridyl rings are not quite coplanar with the central benzene ring, with the angles being 15.99(7), 24.58(6), and 18.91(6)°. As for dpyb-Br, there are also very weak C–H···N interactions [the strongest is C22–H22···N3 = 3.516(2) Å]. In the case of HL⁵, the mesityl group is close

(26) For example, see: (a) Constable, E. C.; Lewis, J.; Liptrot, M. C.; Raithby, P. R. *Inorg. Chim. Acta* **1990**, *178*, 47. (b) Constable, E. C.; Khan, F. A.; Raithby, P. R.; Marquez, V. E. *Acta Crystallogr., Sect. C* **1992**, *C48*, 932.

(27) Leslie, W.; Batsanov, A. S.; Howard, J. A. K.; Williams, J. A. G. *Dalton Trans.* **2004**, 623.

(28) Jones, P. G.; Dubenitschek, P.; Dyker, G.; Nouroozian, M. Z. *Kristallogr.* **1997**, *212*, 87 (CSD No. 402930).

to perpendicular to the central ring with an angle of $80.53(4)^\circ$, as would be expected because of the increased steric bulk of the substituent. However, the pyridyl rings are also more inclined than those in dpyb-Br and HL⁴, with angles of $34.64(6)$ and $30.06(6)^\circ$ between the lateral pyridyl rings and the central benzene ring.

Synthesis and Characterization of Complexes. With the exception of [PtL⁹Cl], all of the complexes were prepared by the reaction of the corresponding ligand with K₂PtCl₄ in acetic acid at reflux under nitrogen, as originally reported by Cárdenas et al. for the parent complex [PtL¹Cl].²⁹ The resultant complexes have relatively low solubility and precipitate from the acetic acid solution. A simple purification procedure (see the Experimental Section) allows the compounds to be isolated in yields typically of around 50–60%. In the case of the pyridyl-appended complex [PtL⁴Cl], a second potential N^C-coordinating binding site for platinum is present, although no evidence for the competitive formation of a dimetallic complex was observed, even in the presence of excess K₂PtCl₄. For the dimethylamino-substituted complex [PtL⁹Cl], an alternative solvent system of acetonitrile/water was employed {3:1 (v/v)}, as used previously for [PtL²Cl]²⁴ to avoid problems associated with the protonation of the pendent amino group of the product that would occur in an acetic acid solution.

Apart from the obvious loss of the H^{2'} resonance (see Scheme 1 for the numbering system), the main systematic changes in the ¹H NMR spectra of the ligands upon coordination to platinum(II) in an N^C^N manner were found to be (i) a shift to high frequency of the H⁶ resonance ($\Delta\delta$ 0.5–0.6 ppm), accompanied by the appearance of well-defined ¹⁹⁵Pt ($I = 1/2$) satellites about this signal (³*J* of ca. 40 Hz), (ii) a shift to low frequency of the H^{4'} resonance of the central ring ($\Delta\delta$ 0.6–0.75 ppm), in some instances accompanied by resolvable ¹⁹⁵Pt satellites (⁴*J* of ca. 6 Hz), and (iii) a small shift of the pyridyl H⁴ resonance to higher frequency ($\Delta\delta$ 0.1–0.2 ppm) and a comparable shift of H³ to lower frequency, the summative effect of which is to lead to a reversal of the ordering of these two signals in the spectra of the complexes compared to those of their respective ligands. The chemical shifts of resonances in the pendent aryl groups were not substantially changed upon coordination, although ¹H–¹H NOESY was again useful for unambiguous assignments.

(a) Crystal Structures of [PtL⁶Cl] and [PtL³Cl]. Single crystals of the biphenyl-substituted complex [PtL⁶Cl] were obtained from a chloroform solution, and the structure was determined using X-ray diffraction. In the crystal structure, the [PtL⁶Cl] molecule lies on a crystallographic 2-fold axis that passes through the metal ion, the chloride ligand, and the cyclometalated carbon (Figure 2a and Table S1 of the Supporting Information). The platinum ion, the three coordinating rings, and the chloride ligand are planar, but the N–Pt–N axis is distorted away from linearity, with an angle of $161.1(1)^\circ$. This reflects the distortion and chelate ring

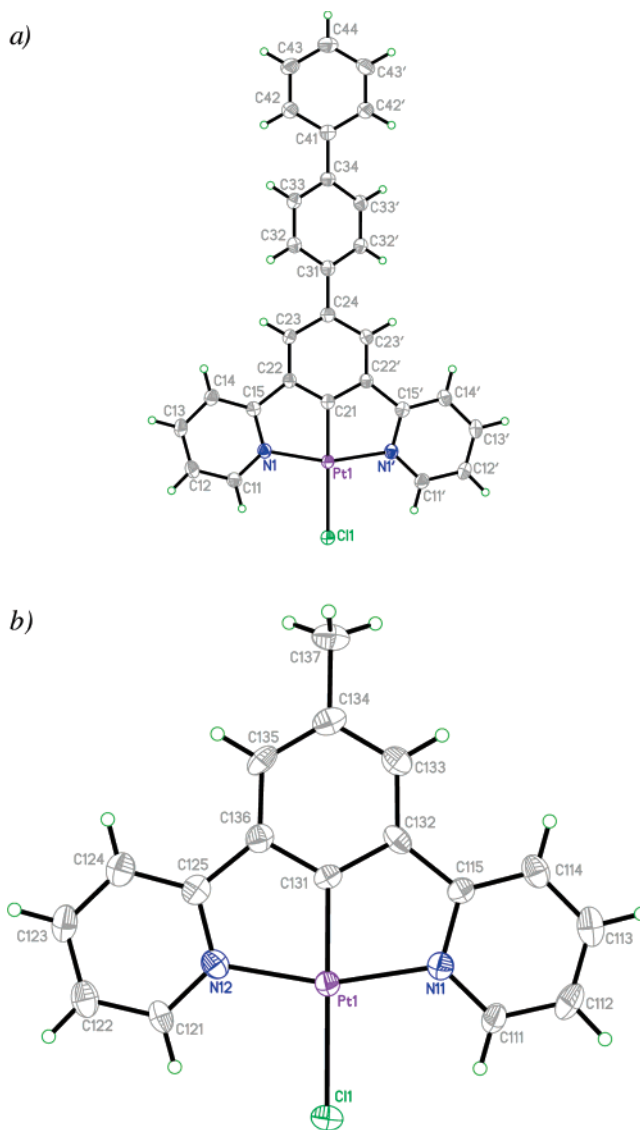


Figure 2. Molecular structures of [PtL⁶Cl] (a) and [PtL³Cl] (b) at 120 K, with displacement ellipsoids at the 50% level. Selected bond lengths (Å) and angles (deg): for [PtL⁶Cl], Pt1–C21 1.912(3), Pt1–N1 2.045(2), Pt1–Cl1 2.422(1), N1–Pt1–N1' 161.13(11); for [PtL³Cl], Pt1–C131 1.908(6)/1.920(6), Pt1–N11 2.044(5)/2.031(5), Pt1–N12 2.033(6)/2.025(5), Pt1–Cl1 2.406(2)/2.416(2), N11–Pt1–N12 161.4(2)/161.6(2).

strain that such ligands suffer when bound terdentately, a feature shared with other transition-metal complexes of terpyridines {e.g., the corresponding angle in [Pt(4-Ph-tpy)-Cl]⁺ is $162.8(4)^\circ$ }.³⁰ This strain is also manifested in the rather compressed angle of $112.6(2)^\circ$ between the central benzene ring and the pyridyl substituents. In all of these features, the structure closely resembles those of [PtL¹Cl] and [PtL²Cl] reported previously.^{24,29} It is significant that the Pt–C bond length [1.912(3) Å] is considerably shorter than that found in complexes incorporating 6-phenyl-2,2'-bipyridine and its derivatives (typically around 2.04 Å), and the Pt–N bond lengths are also somewhat shorter than that for the bond to the lateral nitrogen in the latter class of complexes [2.045(2) Å compared with values of around 2.14 Å³¹]. The angle between the plane of the cyclometalated ring

(29) Cárdenas, D. J.; Echavarren, A. M.; Ramírez de Arellano, M. C. *Organometallics* **1999**, *18*, 3337.

(30) Buchner, R.; Cunningham, C. T.; Field, J. S.; Haines, R. J.; McMillin, D. R.; Summerton, G. C. *J. Chem. Soc., Dalton Trans.* **1999**, 711.

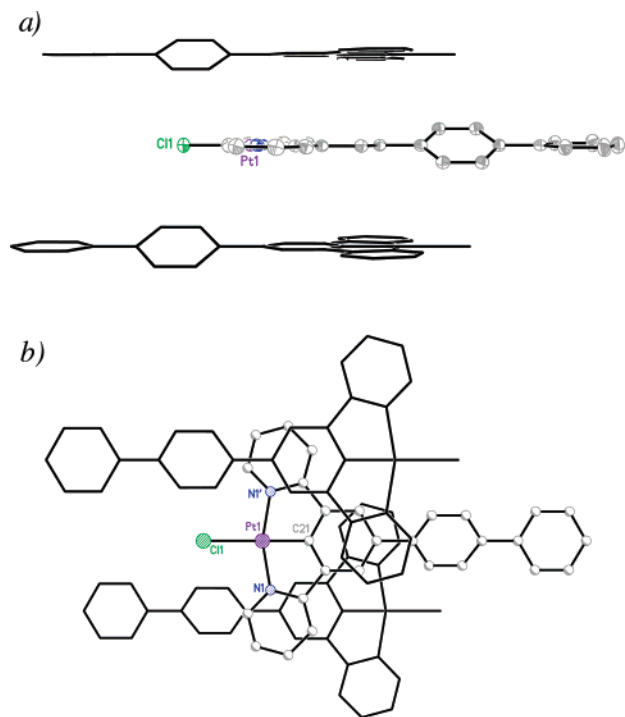


Figure 3. Crystal packing in [PtL⁶Cl] showing the stacking parallel (a) and perpendicular (b) to the Pt(N \wedge C \wedge N)Cl plane.

and that of the first ring of the biphenyl pendent is 29.63(16) $^\circ$, while the angle between the constituent rings of the biphenyl unit is 26.99(19) $^\circ$ in the opposing direction, such that the cyclometalated ring and the terminal ring are almost coplanar [the angle between their planes is only 2.6-(2) $^\circ$]. Twisting about the interannular C–C bonds has similarly been observed by Alcock et al. for a series of 4'-biphenyl-substituted 2,2':6',2''-terpyridyl (biptpy) complexes containing transition-metal ions, M²⁺, with values reported of around 30 $^\circ$.³² The packing of [PtL⁶Cl] can be compared to that seen in the [M(biptpy)₂]²⁺ metal complexes, where four different packing motifs were identified.³² In the case of [PtL⁶Cl], the molecules stack flat in an offset head-to-tail arrangement, similar to the type B stacking reported by Alcock for [Cd(biptpy)₂](PF₆)₂. However, when compared with [Cd(biptpy)₂](PF₆)₂ (where one of the pyridine rings sits above the first of the pendent biphenyl rings), the molecules are laterally further apart, so that the pyridine rings are positioned partially over the cyclometalated ring of the next molecule (Figure 3).

The crystal structure of the methyl derivative [PtL³Cl] has also been determined during this work (Figure 2b and Table S1 in the Supporting Information) and displays bond lengths and angles very similar to those found in the Pt(NCN)Cl core of [PtL⁶Cl] discussed above and in the other crystallographically characterized complexes, [PtL¹Cl] and [PtL²Cl].^{24,29} In this case, two different environments in the crystal were observed, but corresponding bond lengths and angles

are almost all the same (Table S1 in the Supporting Information).

Electrochemistry. Within the range –2.4 to +1.0 V (vs Fc/Fc⁺), all of the complexes show one irreversible reduction process [in 9:1 (v/v) CH₃CN/CH₂Cl₂], at a similar value of around –2.0 V in each case and comparable to that observed for the parent complex (Table 1). The presence of the aryl substituents has only a small and erratic effect on the reduction potential, probably because the lowest unoccupied molecular orbital in these complexes is dominated by the pyridyl rings, with little contribution expected from the formally anionic cyclometalating ring or its pendent aryl substituent.

Complexes [PtL⁴Cl]–[PtL⁷Cl] display one irreversible oxidation wave within this region, while [PtL⁸Cl] and [PtL⁹Cl] also display a second oxidation process. The oxidation potential shows rather more variation with the substituent than the reduction potential (Table 1), suggesting that the central phenyl ring makes a more substantial contribution to the highest occupied molecular orbital (HOMO). The observed order, mesityl > 2-pyridyl > 4-tolyl > 4-biphenyl > methyl > 2-thienyl > 4-(dimethylamino)phenyl, can be rationalized in terms of the electron-withdrawing or -donating ability of the substituents. Thus, in terms of the σ -bonding framework, simple aryl substituents are electron-withdrawing relative to methyl, accounting for the higher E^{ox} values exhibited by the first four complexes listed compared to R = methyl.³³ However, this effect can be offset by donation through the π -bonding framework, which will be most significant for the most conjugated substituent, biphenyl (hence, a lower E^{ox}), and least significant for R = mesityl, where the steric encumbrance associated with the *o*-methyl groups will inhibit the attainment of the coplanar conformation required for efficient conjugation (hence, the highest E^{ox} for this complex). Thiophene is an electron-rich heterocycle, while the dimethylamino substituent is strongly electron-donating through the π framework, accounting for the particularly low E^{ox} values observed for [PtL⁸Cl] and [PtL⁹Cl], respectively. The second oxidation process observed for [PtL⁹Cl] is reversible, $E_{1/2} = 0.29$ V. Because the free ligand HL⁹ also displays a reversible oxidation at only a slightly smaller potential ($E_{1/2} = 0.24$ V), we attribute the second oxidation process in the complex to oxidation of the (dimethylamino)phenyl substituent and the first to the Pt(N \wedge C \wedge N)Cl core of the complex, as for the other compounds.

Photophysical Properties. Absorption and emission data for the complexes prepared in this study are listed in Table 1, together with corresponding values for the three previously studied complexes for comparison.²⁴

Absorption. All of the new complexes display very intense absorption bands below 330 nm, because of $^1\pi-\pi^*$ transi-

(31) A search in the CCD reveals a mean value of 2.04 Å for the Pt–C bond length in six N \wedge N \wedge C complexes, 2.14 Å for the lateral Pt–N bond, and 1.97 Å for the bond to the central N.

(32) Alcock, N. W.; Barker, P. R.; Haider, J. M.; Hannon, M. J.; Painting, C. L.; Pikramenou, Z.; Plummer, E. A.; Rissanen, K.; Saarenketo, P. *J. Chem. Soc., Dalton Trans.* **2000**, 1447.

(33) The opposing effects of σ withdrawal and π donation on the electrochemistry of 4'-aryl-substituted [Pt(N \wedge N \wedge N)Cl] complexes are described in ref 13c. A detailed discussion of similar observations in [Ru(N \wedge N \wedge N)₃]²⁺ complexes is provided by: Damrauer, N. H.; Boussie, T. R.; Devenney, M.; McCusker, J. K. *J. Am. Chem. Soc.* **1997**, *119*, 8253.

Table 1. Photophysical and Electrochemical Data for the Platinum Complexes^{a,c}

complex	substituent	absorbance $\lambda_{\text{max}}/\text{nm}$ ($\epsilon/\text{L mol}^{-1} \text{cm}^{-1}$)	emission $\lambda_{\text{max}}/\text{nm}$	τ_0/ns^b	k_{Q} (self-quenching)/ $10^9 \text{ M}^{-1} \text{ s}^{-1}$	ϕ_{lum} degassed (aerated)	k_{Q} (O_2 quenching)/ $10^8 \text{ M}^{-1} \text{ s}^{-1}$	$E_p^{\text{ox}}/\text{V}^c$	$E_p^{\text{red}}/\text{V}^c$
[PtL ¹ Cl] ^d	H	332 (6510), 380 (8690), 401 (7010), 454 (270), 485 (240)	491, 524, 562	7.2	5.3	0.60 (0.039)	9.1	0.43	-2.03
[PtL ² Cl] ^d	ester	329 (7560), 380 (9990), 397 (7880), 446 (180), 478 (200)	481, 513, 550	8.0	3.6	0.58 (0.067)	4.4	0.47	-1.93
[PtL ³ Cl] ^d	methyl	335 (5710), 381 (6900), 412 (6780), 460 (190), 495 (130)	505, 539, 578	7.8	3.3	0.68 (0.024)	16	0.37	-2.02
[PtL ⁴ Cl]	pyridyl	364 sh (4700), 382 (7510), 412 (7540), 493 (120)	506, 538, 580 (sh)	9.2	4.4	0.57 (0.043)	5.7	0.53	-2.00
[PtL ⁵ Cl]	mesityl	332 sh (5640), 363 (3850), 381 (5410), 410 (5210), 492 (130)	501, 534, 574 (sh)	7.9	1.0	0.62 (0.045)	7.4	0.58	-1.99
[PtL ⁶ Cl]	biphenyl	364 sh (7520), 381 (11500), 418 (12400), 496 (230)	522, 551 (sh)	11.5	6.1	0.65 (0.035)	6.9	0.40	-1.84
[PtL ⁷ Cl]	tolyl	332 sh (4750), 362 sh (3090), 381 (4670), 418 (5020), 496 (140)	516, 544 (sh)	9.2	2.5	0.59 (0.035)	7.8	0.43	-2.00
[PtL ⁸ Cl]	thienyl	363 sh (3270), 380 (4690), 426 (5080)	548, 584, 641 (sh)	20.5	1.1	0.54 (0.015)	7.8	0.23, 0.61	-1.93
[PtL ⁹ Cl]	aminophenyl	380 (6410), 431 (8880)	588	12.4	0.12	0.46 (0.007)	24	0.19, 0.29 ^e	-2.06
[PtL ⁹ HCl] ⁺	aminophenyl-H ⁺	331 sh (8070), 362 (5560), 381 (7720), 410 (7310)	482, 514, 547	5.8	1.5	0.40 (0.041)	6.8		

^a In dichloromethane at 295 K, except where stated otherwise. ^b Lifetime at infinite dilution. ^c In $\text{CH}_3\text{CN}/\text{CH}_2\text{Cl}_2$ [9:1 (v/v)], in the presence of 0.1 M $[\text{Bu}_4\text{N}][\text{BF}_4]$ as the supporting electrolyte; scan rate 300 mV s^{-1} ; all processes were chemically irreversible, except for that indicated with footnote e); $E_p^{\text{ox/red}}$ = peak potential of chemically irreversible oxidation/reduction; values are reported vs Fc^+/Fc ($E_{1/2} = +0.42 \text{ V}$ vs SCE). ^d Absorption and emission data from ref 24. ^e Chemically reversible process; anodic-to-cathodic peak separation, $\Delta E = 90 \text{ mV}$; the quoted value is the half-wave potential. For HL⁹, $E_{1/2} = 0.26 \text{ V}$ and $\Delta E = 70 \text{ mV}$.

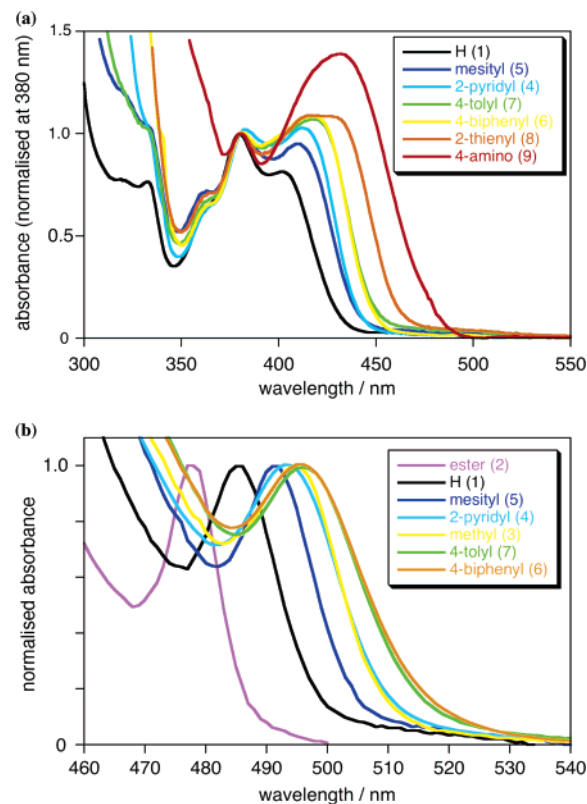


Figure 4. (a) UV-visible absorption spectra of the platinum(II) complexes in a dichloromethane solution at 295 K, normalized at 380 nm for comparison (extinction coefficients are given in Table 1). (b) Expansion of the low-energy region, showing the weak bands attributed to direct population of ³LC excited states.

tions localized on the ligands ($\epsilon > 20\,000 \text{ L mol}^{-1} \text{ cm}^{-1}$), together with a set of intense bands in the region 350–430 nm ($\epsilon = 5000\text{--}10\,000 \text{ L mol}^{-1} \text{ cm}^{-1}$; Figure 4a). The latter comprise at least three bands, of which the position of one, at 380 (± 1) nm, is the same in each complex and hence must arise from a transition that is independent of the 5' substituent. On the other hand, the component band at lowest energy is increasingly red-shifted from 401 to 431 nm in the order mesityl < 2-pyridyl < 4-tolyl = 4-biphenyl < 2-thienyl < 4-dimethylamino (values in CH_2Cl_2). This order correlates with the decreasing order of the oxidation potentials of the complexes discussed above. In fact, the absorption energy (E_{abs}) increases linearly with an increase in the oxidation potential, at a rate of $2900 \text{ cm}^{-1} \text{ V}^{-1}$ (see Figure S1 in the Supporting Information for a plot of E_{abs} vs E^{ox}), confirming the influence of the substituent on the HOMO energy. For each complex, this band displays significant negative solvatochromism, typically increasing in energy by around 1500 cm^{-1} on going from the least polar solvent investigated, CCl_4 , to the most polar solvent, CH_3CN . Absorption data for all of the complexes in a range of solvents are provided in Table S3 in the Supporting Information. Such behavior is typical of transitions with an appreciable degree of charge-transfer character and, normally, to an excited state of lower dipole moment than the ground state.³⁴

A much weaker band ($\epsilon \approx 200 \text{ L mol}^{-1} \text{ cm}^{-1}$) is discernible at lower energy for all of the complexes (Figure

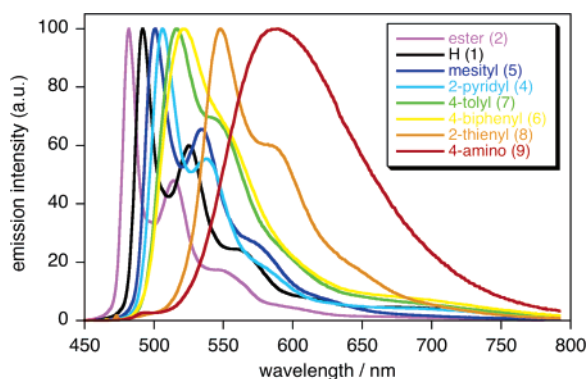


Figure 5. Emission spectra of the complexes in a dilute solution (10^{-5} M) in dichloromethane at 295 K ($\lambda_{\text{ex}} = 400$ nm; band-passes of 1.0 nm).

4b), except for the thienyl and amino compounds, where it may be obscured by the tail of the charge-transfer band. The wavelength of this band is very similar in each case (492–496 nm), comparable to that for the methyl-substituted compound (495 nm), and displays a much weaker degree of solvatochromism than the intense charge-transfer band. This band is attributed to the direct population of states of primarily ^3LC character, facilitated by the high spin–orbit coupling associated with the platinum(II) ion.^{24,35}

Emission. All of the complexes studied are intensely luminescent in solution at room temperature (Figure 5 and Table 1). The luminescence quantum yields in a degassed dichloromethane solution are on the order of 0.5–0.6 in each case, values which are particularly high among the numerous luminescent platinum(II) complexes reported to date. The emission spectra of $[\text{PtL}^1\text{Cl}]$ – $[\text{PtL}^8\text{Cl}]$ are highly structured, typical of luminescence from states of primarily ^3LC character. The component band of highest intensity is the one of highest energy (i.e., the 0–0 transition), indicating a minimal difference in geometry between the ground and excited electronic states; the Stokes shifts are small; and the spectra show only very weak negative solvatochromism (e.g., shifting by only 200–250 cm^{-1} on going from CH_3CN to CCl_4 ; see Table S3 in the Supporting Information for data). These are all further features that are typically more characteristic of ligand-centered, as opposed to charge-transfer, states. The amino-substituted complex $[\text{PtL}^9\text{Cl}]$ is anomalous in this respect, displaying a broad structureless emission band and strong positive solvatochromism. Its behavior will be discussed separately.

The emission maxima are increasingly red-shifted by the substituent in the order mesityl < 2-pyridyl < 4-tolyl < 4-biphenyl < 2-thienyl. Again, the emission energy, E_{em} , correlates roughly linearly with the oxidation potential (Figure S2 in the Supporting Information), in line with the influence of the aryl substituents on the energy of the HOMO. However, at 4900 cm^{-1} V^{-1} , the dependence is markedly steeper than that observed for the absorption band, consistent with a different nature to the emissive state

(34) A detailed discussion of this effect in platinum(II) diimine complexes is provided by: Cummings, S. D.; Eisenberg, R. *J. Am. Chem. Soc.* **1996**, *118*, 1949. See also ref 23.

(35) Zheng, G. Y.; Rillema, D. P.; DePriest, J.; Woods, C. *Inorg. Chem.* **1998**, *37*, 3588.

compared to that formed initially upon excitation into the strong, solvatochromic absorption band. We have previously observed a similar ordering (H \approx mesityl < ω -pyridyl < 4-tolyl < 4-biphenyl) in the ^3LC emission of a series of 4'-substituted bis(terpyridyl)iridium(III) complexes.²⁷

As described in the previous section, the lowest-energy band in the absorption spectra, attributed to direct excitation to the ^3LC state, occurs at almost the same wavelength for all of the aryl-substituted complexes (494 ± 2 nm). Hence, given the trend in the emission energy, there is a clear, progressive increase in the Stokes shift between the ^3LC absorption band and the emission band (0–0 transition) in the same order: H < mesityl < 2-pyridyl < 4-tolyl < 4-biphenyl < 2-thienyl. Presumably, this arises from the need for torsional rearrangement to occur following light absorption for maximal conjugation of the aryl substituent with the N[^]C[^]N core. An approximately coplanar conformation of the pendent and cyclometalating rings will be required to maximize the conjugation in the excited state, whereas in the initially formed conformation of the excited state, the mean dihedral angle is expected to be larger, similar to that in the ground state (e.g., around 30° according from the X-ray structure of $[\text{PtL}^6\text{Cl}]$). To verify this hypothesis, measurements in a frozen glass at 77 K have been performed, where torsional rearrangement is inhibited. The spectrum of the mesityl-substituted complex at 77 K [2:2:1 (v/v) ether/isopentane/ethanol] is unchanged compared to the room-temperature spectrum, whereas the emission maxima of the other complexes are blue-shifted by 5–10 nm, consistent with the requirement for a change in the conformation for maximal conjugation to be attained.

(a) Concentration Dependence, Self-Quenching, and Excimer Formation. For the complexes $[\text{PtL}^1\text{Cl}]$ – $[\text{PtL}^8\text{Cl}]$, increasing the concentration leads to the appearance of a new, broad, structureless emission band centered at 690–700 nm, which becomes progressively more intense at the expense of the shorter wavelength bands.³⁶ This is characteristic of excimer formation and emission.³⁷ The temporal decay of the emission registered in the region of monomer luminescence (480–550 nm), where no contribution from the excimer is anticipated, remains monoexponential over the whole range of concentrations studied (7.5×10^{-6} – 1.5×10^{-4} M). In contrast, the emission kinetic trace registered at 680 nm shows a monoexponential growth of the emission intensity ($k_{\text{obs}} \approx 10^6 \text{ s}^{-1}$) as the excimer responsible for the emission at this wavelength is formed from the monomer, followed by a monoexponential decay with the same rate constant as that of the monomer. The observed emission

(36) No significant differences were observed in the position or spectral profile of the excimer formed by the different aryl-substituted complexes, being effectively identical with that reported previously for $[\text{PtL}^1\text{Cl}]$.²⁵

(37) Many square-planar platinum(II) complexes are subject to self-quenching, owing to attractive intermolecular interactions between the excited state and its ground-state analogue. Only in some cases, however, is excimer emission detectable, for example, in $[\text{Pt}(\text{diimine})(\text{CN})_2]$ complexes² and, though to a lesser extent, certain $[\text{Pt}(\text{phen})(\text{acetylide})_2]$ systems.³ Cyclometalated complexes (e.g., those of phbpy) usually display self-quenching that is not accompanied by detectable excimer emission.⁶

decay rate constants (k_{obs}) increase linearly with the concentration, fitting well to an expression of the form

$$k_{\text{obs}} = k_0 + k_{\text{Q}}[\text{Pt}] \quad (1)$$

where k_0 is the emission rate constant at infinite dilution and k_{Q} is an apparent rate constant of self-quenching.^{2,3,38} This latter parameter has been shown to be determined by the product of the equilibrium constant for excimer formation (K_{E}) and the sum of the rate constants of the radiative and nonradiative decay pathways of the excimer.^{2,38} Thus, k_{Q} provides an indication of the susceptibility of the complex to self-quenching through excimer formation.

Values of k_0 and k_{Q} have been determined for each complex in this way from measurements of k_{obs} over a range of concentrations. The lifetimes of emission at infinite dilution τ_0 listed in Table 1 are the values of $1/k_0$. The lifetimes are all similar to one another and to that of the parent complex (around 8 μs), with the exception of the thienyl-substituted complex, which has a significantly longer lifetime of 21 μs (values in degassed dichloromethane at room temperature). The lifetimes at 77 K [2:2:1 (v/v) ether/isopentane/ethanol] were the same, within the experimental uncertainty on the measurement, as those determined at room temperature, a remarkable testament to the success of the N \wedge C \wedge N coordination in eliminating all pathways of potential thermally activated nonradiative decay.

The complexes reveal considerable variation in the value of k_{Q} (Table 1). The introduction of aryl substituents into the 5' position of the ligand might be expected to reduce the tendency to form excimers compared to the parent complex, owing to steric inhibition by the pendent aryl group preventing the necessary face-to-face approach of a complex in its excited state to a ground-state molecule. This prediction was borne out by most of the new complexes, and there is evidence for a trend in k_{Q} with respect to the increasing steric demand of the substituent. Thus, k_{Q} is reduced from $3.3 \times 10^9 \text{ M}^{-1} \text{ s}^{-1}$ in the methyl-substituted complex to $2.5 \times 10^9 \text{ M}^{-1} \text{ s}^{-1}$ in the tolyl-substituted analogue and further reduced in the most sterically encumbered mesityl system to $1.0 \times 10^9 \text{ M}^{-1} \text{ s}^{-1}$. The values for the biphenyl and thienyl complexes lie between those of the tolyl and mesityl compounds. On the other hand, the pyridyl substituent in [PtL⁴Cl] might reasonably be expected to have a steric influence comparable to that of a tolyl group, yet k_{Q} for this complex is actually higher than that for the simple, methyl-substituted complex. Clearly, steric effects are only part of the picture, and the electronic influence of the substituent must also play a role in determining the affinity of the excited-state molecule for a ground-state molecule. An interesting question pertaining to excimer formation in platinum diimine complexes is the nature of the attractive interactions, e.g., Pt–Pt or ligand–ligand or combinations of these.² That excimer formation in the present set of aryl complexes occurs at all, and is relatively significant even in the presence of sterically demanding substituents in the ligands, may suggest that a head-to-tail interaction is

primarily responsible here, where the aryl groups would be disposed on opposite sides of the dimer.

Efficient quenching of the emission of each complex by dissolved molecular oxygen is observed, with quenching rate constants close to $10^9 \text{ M}^{-1} \text{ s}^{-1}$ (Table 1).

(b) Emission Properties of the Amino-Substituted Complex [PtL⁹Cl]. This complex, which carries a 4-(dimethylamino)phenyl substituent at the 4 position of the N \wedge C \wedge N core, exhibits very different luminescence properties from all of the other complexes in a dichloromethane solution (Figure 5). (i) The emission band at room temperature is broad (half-height width of 120 nm) and unstructured. (ii) The emission is substantially red-shifted compared to the other compounds ($\lambda_{\text{max}} = 588 \text{ nm}$ in CH_2Cl_2): the position of this complex in the plot of E_{em} vs E^{ox} is anomalous (see Figure S2 in the Supporting Information). (iii) The complex is subject to very little self-quenching: the apparent rate constant of self-quenching k_{Q} ($\approx 0.12 \times 10^9 \text{ M}^{-1} \text{ s}^{-1}$) is approximately 20 times smaller than that for the tolyl-substituted complex. (iv) The emission in this complex is substantially more sensitive to oxygen than in all of the other complexes; for example, the emission quantum yield is reduced by a factor of 65 in an aerated versus degassed solution in CH_2Cl_2 (Table 1).

These differences suggest a switch in the nature of the lowest excited state from ³LC in [PtL^{1–8}Cl] to one of primarily ILCT character in the amino complex [PtL⁹Cl]. It is likely that the introduction of the strongly electron-donating Me₂N– substituent raises the energy of the pendent aryl group to such an extent that there is a high-energy molecular orbital localized predominantly on this group, and the lowest-energy excited state corresponds to an ILCT ($\pi_{\text{Me}_2\text{N-Ar}} - \pi_{\text{NCN}}^*$) transition rather than the locally excited states ($\pi_{\text{NCN}} - \pi_{\text{NCN}}^*$) of the other complexes. The electrochemical data for this complex lend support to this hypothesis: the Me₂N–C₆H₅– group displays an oxidation potential only slightly higher than that of the Pt(N \wedge C \wedge N)Cl core, as discussed earlier. A related effect has been observed by McMillin and co-workers in a series of [Pt(X-tpy)Cl]⁺ complexes, where X-tpy is a 4'-substituted terpyridine ligand: the introduction of increasingly electron-donating substituents, such as –NMe₂ or pyrene, leads to an increase in the contribution of ILCT character in the emissive state.¹³ Similarly, we recently observed a switch in the nature of the lowest-energy excited state from ³LC to ILCT in bis(terpyridyl)iridium(III) complexes, upon the introduction of a –C₆H₄–NMe₂ substituent into the terpyridine.³⁹ Notably, the luminescence quantum yield of [PtL⁹Cl] is again very high ($\phi = 0.46$), despite the lower energy of the excited state.

Further evidence in support of the charge-transfer assignment in a dichloromethane solution is provided by the very pronounced positive solvatochromism in the emission spectrum of this complex (Figure 6). For example, the emission energy is almost 4000 cm^{-1} lower in CH_3CN than in CCl_4 . In fact, the spectrum in the least polar solvent investigated,

(38) Horvath, A.; Stevenson, K. L. *Coord. Chem. Rev.* **1996**, *153*, 57.

(39) Leslie, W.; Poole, R. A.; Murray, P. R.; Yellowlees, L. J.; Beeby, A.; Williams, J. A. G. *Polyhedron* **2004**, *23*, 2769.

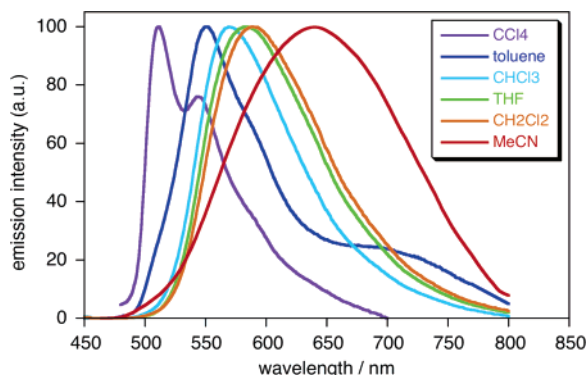


Figure 6. Emission spectra of [PtL⁹Cl] at 295 K in several solvents of differing polarity, showing the strong positive solvatochromism. Note the change to a structured, high-energy emission spectrum in CCl₄, resembling that displayed by the other complexes, and the presence of excimer emission in toluene at the concentration employed (10⁻⁴ M).

CCl₄, resembles the spectra of the other complexes, displaying structured emission and with an emission maximum similar to that of the pyridyl-substituted complex. Thus, we conclude that the ³LC and ILCT states are close in energy in [PtL⁹Cl]. In the least polar solvents, the former is the lower in energy and structured emission is observed. In more polar solvents, the ILCT energy is reduced, owing to the high degree of charge separation, to such an extent that in CH₂-Cl₂ and CH₃CN it is lower in energy than the ³LC. The trend is thus reminiscent of the classical behavior of organic molecules such as 4-(dimethylamino)benzointrile that may display either localized or twisted intramolecular charge-transfer emission, according to the environment.⁴⁰

The ILCT character of the lowest excited state in CH₂Cl₂ might also account for the greatly attenuated self-quenching and absence of excimer formation for [PtL⁹Cl] in this solvent because the excited state will have lower affinity for a ground-state molecule, which plays the role of a Lewis base in the process of excimer formation. A somewhat analogous effect has been reported by McMillin and co-workers in their study of 4'-aryl-substituted terpyridylplatinum complexes, where the increasing ILCT character correlated well with a systematic moderation of exciplex quenching by, for example, butyronitrile.¹³ If such an explanation indeed applies in the present instance, then excimer formation might be predicted in CCl₄, in which solvent the emissive excited state has ³LC character, as discussed above. Unfortunately, the complex has poor solubility in this solvent, and concentrations sufficient for excimer emission to be observed are not achievable. However, a saturated solution in toluene does show clear evidence of excimer emission (Figure 6). Toluene is probably sufficiently nonpolar to ensure that the ³LC state remains lower in energy.

(c) Effect of Protonation of the Pendent Amine. Protonation of [PtL⁹Cl] in CH₂Cl₂ by the addition of trifluoroacetic acid results in a dramatic set of changes in the absorption and luminescence properties (Figure 7 and Table 1). The emission maximum is blue-shifted by 3700 cm⁻¹, the spectrum becomes more structured, self-quenching and

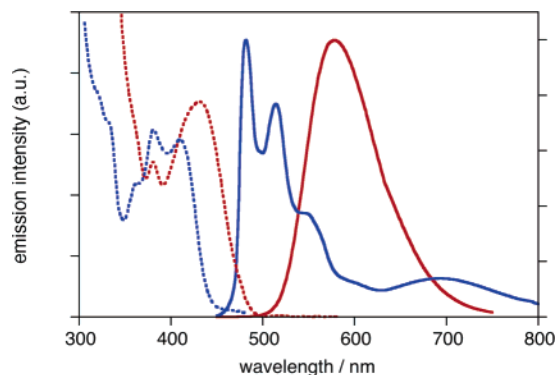


Figure 7. Emission and excitation spectra of [PtL⁹Cl] in CH₂Cl₂ (6.0 × 10⁻⁵ M) at 295 K (red solid and dotted lines, respectively), and the corresponding blue-shifted spectra (in blue), after the addition of trifluoroacetic acid (10⁻² M). λ_{ex} = 408 nm in both cases (isosbestic point); λ_{em} = 588 and 488 nm, respectively; band-passes = 2 nm. Note the appearance of an excimer band for the protonated complex.

excimer formation at elevated concentrations become significant, and the limiting lifetime in a dilute solution is shortened by a factor of 2. These changes in emission are accompanied by a blue shift of the intense charge-transfer band in absorption (Figure 7). All of these effects are consistent with a switch in the nature of the lowest-energy excited state from the ILCT character of [PtL⁹Cl] to the ³-LC character observed for all of the other complexes, which can be attributed directly to the removal of the influence of the electron-donating amino group upon protonation. Indeed, the spectral parameters for [PtL⁹HCl]⁺ are very similar to those of the mesityl-substituted complex [PtL⁵Cl], in line with the presence of a pendent aryl group that now has little influence. The luminescence quantum yield remains high (φ = 0.40). The lower value of k_Q for [PtL⁹HCl]⁺ than, for example, the tolyl-substituted complex [PtL⁷Cl], can be attributed to the net positive charge of the former, which should disfavor the close approach of the excited- and ground-state molecules. On the other hand, the fact that excimer formation remains quite significant, despite the positive charge, again supports the notion that a head-to-tail disposition of the two complexes in the excited-state dimer is more likely.

This protonation-induced switching between two different types of excited states with significantly different energies, *both of which are highly emissive*, is an unusual feature. Several platinum group metal complexes incorporating amino or pyridyl functionality in one or more of the ligands display luminescence, which can be modulated through protonation of the nitrogen atom.⁴¹ However, in most cases, one or the other of the two forms is quenched, and the effect is usually a change in the intensity of the emission, as opposed to the emission energy. The effect of protonation is fully reversible upon the addition of a stoichiometric amount of base required for neutralization, and the complex [PtL⁹Cl] is stable in the presence of larger amounts of base (e.g., no significant decomposition was observed in the presence of 0.2 M Et₃N

(40) Rettig, W. *Angew. Chem., Int. Ed.* **1986**, *25*, 971.

(41) For a recent example involving platinum complexes, see: Yang, Q.-Z.; Tong, Q.-X.; Wu, L.-Z.; Wu, Z.-X.; Zhang, L.-P.; Tung, C.-H. *Eur. J. Inorg. Chem.* **2004**, 1948 and ref 14b.

over a period of several hours). In principle, the switching effect observed here could be utilized as a component of a sensory system for ratiometric sensing, given that both the emission and excitation spectra are substantially shifted.

Conclusion

In summary, this study demonstrates the versatility of terdentate, N³C¹N-coordinating ligands, based on the 1,3-di(2-pyridyl)benzene structure, for obtaining highly luminescent, cyclometalated platinum(II) complexes. In particular, the introduction of aryl substituents into the 5 position of the benzene ring of the ligand has several important implications. First, it allows the emission wavelength to be tuned over a wide range across the visible region, from 481 nm ([PtL²Cl]) to 640 nm ([PtL⁹Cl]) in CH₃CN (an energy range of 5000 cm⁻¹) while retaining the outstandingly high luminescence quantum yields of 50–60%. Second, the presence of aryl substituents in the complexes diminishes their propensity for self-quenching at elevated concentrations. Finally, the introduction of the strongly electron-donating 4-(dimethylamino)phenyl group leads to a switch in the nature of the lowest excited state to one of primarily ILCT character in polar solvents, while in nonpolar solvents, the ³LC remains lower in energy. Moreover, protonation of the amine also leads to reversible switching to the ³LC state, manifested as a dramatic change in emission maxima from 588 to 482 nm.

Highly emissive, charge-neutral platinum group metal complexes may be suitable for applications as triplet-harvesting agents in OLEDs, and indeed a very recent study has shown excellent results for [PtL³Cl] in a polymer-based device.⁴² Thus, the availability of a family of complexes with tunable emission over a wide range offers considerable scope in the further development of this field. The effect of the aryl substituents in reducing self-quenching is also an attractive feature for practical applications such as OLED technology, where local concentrations may be quite high, and self-quenching is a wasteful energy sink that diminishes device efficiencies. Finally, the sensitive solvent dependence of the emission of [PtL⁹Cl], and the protonation-induced switching between excited states in this complex, could form the basis of novel sensory systems for a variety of species through incorporation of the amine into an appropriate receptor.

Experimental Section

Synthetic Details. ¹H and ¹³C NMR spectra, including NOESY and COSY, were recorded on a Varian 400- or 500-MHz instrument and referenced to residual protiosolvent resonances. Coupling constants are in Hertz. Electrospray ionization (EI) mass spectra of ligands were acquired on a time-of-flight Micromass LCT spectrometer; high-resolution spectra for accurate mass determinations were also carried out on this instrument. The mass spectra of the complexes were recorded at the EPSRC National Mass Spectrometry Service Centre, Swansea, U.K., using electrospray, fast atom bombardment, or liquid secondary ion mass spectrometry (LSIMS)

ionization, as indicated. All solvents used in preparative work were at least Analar grade, and water was purified using the Purite system. Solvents used for optical spectroscopy were high-performance liquid chromatography grade.

Ligand Prepared Using Route A: 1,3,5-Tris(2-pyridyl)benzene (HL⁴). Toluene (15 mL) was added to a mixture of tbb (0.87 g, 2.76 mmol), 2-(tri-*n*-butylstannyl)pyridine (4.34 g of 81% purity, equivalent to 9.55 mmol, remainder mostly tetra-*n*-butyltin), lithium chloride (1.21 g, 38.6 mmol), and bis(triphenylphosphine)palladium(II) chloride (154 mg, 0.22 mmol) contained in an oven-dried Schlenk tube. The mixture was degassed via five freeze–pump–thaw cycles and then heated at reflux under an atmosphere of dinitrogen for 20 h. A saturated aqueous solution of potassium fluoride (10 mL) was then added to the solution, after cooling to ambient temperature, and stirred for 1 h. The insoluble residue formed was removed by filtration and washed with toluene. The toluene was removed from the combined filtrate and washings under reduced pressure, giving a crude product, which was taken up into dichloromethane (150 mL) and washed with aqueous NaHCO₃ (5% by mass, 2 × 100 mL). The organic phase was dried over anhydrous potassium carbonate and evaporated to dryness. The brown residue was purified by chromatography on silica gel, gradient elution from 100% hexane to 100% diethyl ether, giving HL⁴ as an off-white solid (470 mg, 55%). ¹H NMR (400 MHz, CDCl₃): δ 8.75 (3H, d, ³J = 4.5 Hz, H⁶), 8.74 (3H, s, H²), 7.99 (3H, dd, ³J = 7.5 Hz, ⁴J = 1.0 Hz, H³), 7.81 (3H, td, ³J = 7.5 Hz, ⁴J = 2.0 Hz, H⁴), 7.29 (3H, ddd, ³J = 7.5 and 4.5 Hz, ⁴J = 1.0 Hz, H⁵). ¹³C NMR (CDCl₃): δ 157.1 (quat), 149.7 (C²), 140.5 (quat), 137.1 (C⁴), 126.3 (C⁶), 122.6 (C⁵), 121.2 (C³). MS (ES⁺): *m/z* 310 [M + H⁺]. ¹H NMR data are consistent with values previously reported in CD₂-Cl₂ for this compound, obtained as a side product from the reaction of 2-ethynylpyridine with CpCo(PPh₃)₂.⁴³

Ligands Prepared Using Route B. (a) Bromo-Substituted Intermediate: dpyb-Br. The method employed was similar to that described above for HL⁴, but in this case, only 2.2 equiv of the pyridylstannane was used. Thus, a mixture of tbb (1.43 g, 4.55 mmol) and 2-(tri-*n*-butylstannyl)pyridine (4.10 g of 90% purity, equivalent to 10.03 mmol) was stirred in toluene (15 mL) at reflux under nitrogen, in the presence of lithium chloride (1.56 g, 36.7 mmol) and bis(triphenylphosphine)palladium(II) chloride (191 mg, 0.27 mmol), for 20 h. Workup as above led to a pale-brown residue, which was purified by chromatography on silica gel, gradient elution from hexane to 50% hexane/50% diethyl ether, giving dpyb-Br as a colorless solid (740 mg, 52%). ¹H NMR (400 MHz, CDCl₃): δ 8.72 (2H, dd, ³J = 5.0 Hz, ⁴J = 1.5 Hz, H⁶), 8.55 (1H, t, ⁴J = 1.5 Hz, H⁴), 8.22 (2H, d, ⁴J = 1.5 Hz, H²), 7.80 (4H, m, H³, H⁴), 7.28 (2H, ddd, ³J = 6.5 and 5.0 Hz, ⁴J = 1.5 Hz, H⁵). ¹³C NMR (CDCl₃): δ 155.8 (quat), 149.9 (quat), 141.7 (quat), 137.1 (C⁴), 130.5 (C²), 124.2 (C⁶), 123.7 (C⁴), 123.0 (C⁵), 120.9 (C³). MS (ES⁺): *m/z* 311.0205 [M + H⁺]; calcd for C₁₆H₁₂N₂Br, 311.0184. A small amount of 1,3-dibromo-5-(2-pyridyl)benzene was also isolated at lower polarity (104 mg, 10%).

(b) 5-Mesityl-1,3-di(2-pyridyl)benzene (HL⁵). Dimethoxyethane (10 mL) was added to a mixture of dpyb-Br (208 mg, 0.67 mmol), (2,4,6-trimethylphenyl)boronic acid (121 mg, 0.74 mmol), and Ba(OH)₂·8H₂O (632 mg, 2.00 mmol) in an oven-dried Schlenk tube. The mixture was degassed via three freeze–pump–thaw cycles and placed under nitrogen. Tetrakis(triphenylphosphine)palladium(0) (23 mg, 0.02 mmol) was added under a flow of nitrogen and the mixture heated at reflux (85 °C) under a nitrogen

(42) Sotoyama, W.; Satoh, T.; Sawatari, N.; Inoue, H. *Appl. Phys. Lett.* **2005**, *86*, 153505.

(43) Wakatsuki, Y.; Yoshimura, H.; Yamazaki, H. *J. Organomet. Chem.* **1989**, *366*, 215.

atmosphere for 24 h. The solvent was then removed under reduced pressure and the crude residue taken up into dichloromethane (50 mL) and NaHCO₃ (5% by mass, 50 mL). The organic layer was separated, washed with NaHCO₃ (2 × 50 mL), and dried over anhydrous K₂CO₃. The solvent was removed under reduced pressure, and the pale-brown residue was recrystallized from ethanol to give off-white crystals of the desired product (27 mg, 12%). ¹H NMR (300 MHz, CDCl₃): δ 8.74 (2H, d, ³J = 6.0 Hz, H⁶), 8.69 (1H, t, ⁴J = 1.5 Hz, H²), 7.85 (4H, m, H³, H⁴), 7.77 (2H, td, ³J = 7.5 Hz, ⁴J = 1.8 Hz, H⁴), 7.26 (2H, m, H⁵), 6.97 (2H, s, H^a), 2.35 (3H, s, *p*-CH₃), 2.09 (6H, s, *o*-CH₃). ¹³C NMR (CDCl₃): δ 157.4 (quat), 149.9 (quat), 142.4 (quat), 140.3 (quat), 138.8 (quat), 137.0 (C⁴), 136.9 (quat), 136.2 (quat), 128.7 (C⁵), 128.3 (C⁴), 124.2 (C²), 122.7 (C⁵), 121.0 (C³), 21.2 (*p*-CH₃), 21.1 (*o*-CH₃). MS (ES⁺): *m/z* 351.1852 [M + H⁺]; calcd for C₂₅H₂₃N₂, 351.1856. Anal. Calcd for C₂₅H₂₂N₂: C, 85.68; H, 6.33; N, 7.99. Found: C, 85.58; H, 6.30; N, 7.90.

(c) **5-(4-Biphenyl)-1,3-di(2-pyridyl)benzene (HL⁶)**. 4-Biphenylboronic acid (96 mg, 0.49 mmol) and dpyb-Br (134 mg, 0.43 mmol) were suspended in dimethoxyethane (3 mL), and an aqueous solution of sodium carbonate (137 mg, 1.29 mmol in 0.5 mL water) was added. The mixture was degassed via four freeze–pump–thaw cycles and placed under dinitrogen, and tetrakis(triphenylphosphine)palladium(0) was added (30 mg, 0.03 mmol). The mixture was stirred at room temperature for 1 h before being heated at 80 °C for 67 h. The solvent was then removed and the residue taken up into dichloromethane (50 mL). After washing with water (4 × 50 mL), the organic phase was dried over anhydrous potassium carbonate and the solvent removed under reduced pressure. The beige residue was purified by chromatography on silica gel, gradient elution from hexane to 50% hexane/50% diethyl ether, leading to a colorless solid (80 mg, 48%). ¹H NMR (500 MHz, CDCl₃): δ 8.78 (2H, dd, ³J = 5.0 Hz, ⁴J = 1.0 Hz, H⁶), 8.65 (1H, t, ⁴J = 1.5 Hz, H²), 8.40 (2H, d, ⁴J = 1.5 Hz, H⁴), 8.01 (2H, d, ³J = 8.0 Hz, H³), 7.89 (4H, m, H^a, H⁴), 7.73 (2H, d, ³J = 8.0 Hz, H^b), 7.67 (2H, dd, ³J = 8.0 Hz, ⁴J = 1.0 Hz, H^b), 7.48 (2H, t, ³J = 8.0 Hz, H^a), 7.36 (3H, m, H^c, H⁵). ¹³C NMR (CDCl₃): δ 156.7, 142.3, 140.8, 140.7, 139.6, 138.0, 129.0 (C^a), 128.0 (C^a), 127.7 (C^b), 127.6 (C^c), 127.2 (C^b), 126.9 (C⁴), 125.0, 122.9 (C⁵), 121.6 (C³). MS (ES⁺): *m/z* 385 [M + H⁺]; 385.1694 [M + H⁺]; calcd for C₂₈H₂₁N₂, 385.1699, 407.1514 [M + Na⁺]; calcd for C₂₈H₂₀N₂²³Na, 407.1519. Anal. Calcd for C₂₈H₂₀N₂: C, 87.47; H, 5.24; N, 7.28. Found: C, 86.77; H, 5.22; N, 7.14.

Dibrominated Precursors for Ligands Prepared Using Route C.

(a) **5-(4-Tolyl)-1,3-dibromobenzene**. tbb (2.11 g, 6.69 mmol), *p*-tolylboronic acid (1.00 g, 7.36 mmol), and dimethoxyethane (25 mL) were placed in an oven-dried Schlenk tube, and sodium carbonate (2.13 g, 20.1 mmol), dissolved in the minimum volume of water, was added. The solution was degassed via three freeze–pump–thaw cycles and placed under nitrogen. Tetrakis(triphenylphosphine)palladium(0) (0.23 g, 0.20 mmol) was added under a flow of nitrogen and the mixture heated at reflux for 18 h. The residue obtained upon removal of solvent was taken up into a mixture of dichloromethane (50 mL) and water (50 mL), and the organic layer was separated and washed with more water (3 × 50 mL). After drying of the organic phase over anhydrous magnesium sulfate, the solvent was removed under reduced pressure. The pale-brown residue was purified by column chromatography on silica gel, eluting with hexane, to afford the required product (*R_f* = 0.8 on TLC in hexane) as a colorless solid (650 mg, 29%). ¹H NMR (400 MHz, CDCl₃): δ 7.56 (2H, d, ⁴J = 2.0 Hz, H⁴), 7.53 (1H, t, ⁴J = 2.0 Hz, H²), 7.35 (2H, dd, ³J = 8.0 Hz, H^b), 7.18 (2H, d, ³J = 8.0 Hz, H^a), 2.32 (3H, s, CH₃). MS (EI): *m/z* 326 (M⁺). Among

eluted products of higher polarity was 1-bromo-3,5-di(4-tolyl)benzene (*R_f* = 0.5), also a colorless solid (430 mg, 19%). ¹H NMR (400 MHz, CDCl₃): δ 7.67 (3H, m, H², H⁴, H⁶), 7.51 (2H, d, ³J = 8.0 Hz, H^b), 7.27 (4H, d, ³J = 8.0 Hz, H^a), 2.41 (6H, s, CH₃).

(b) **5-(2-Thienyl)-1,3-dibromobenzene**. This compound was prepared by a procedure similar to that above, starting from tbb (2.24 g, 7.10 mmol) and 2-thiophenylboronic acid (1.00 g, 7.81 mmol) in dimethoxyethane (25 mL). After refluxing for 18 h, a similar workup followed by purification by column chromatography on silica gel, eluting with hexane, gave the required product (*R_f* = 0.7 in hexane) as a colorless solid (870 mg, 39%). ¹H NMR (400 MHz, CDCl₃): δ 7.66 (2H, d, ⁴J = 2.0 Hz, H⁴), 7.56 (1H, t, ⁴J = 2.0 Hz, H²), 7.34 (1H, dd, ³J = 5.0 Hz, ⁴J = 1.0 Hz, H^a), 7.31 (1H, dd, ³J = 3.5 Hz, ⁴J = 1.0 Hz, H^c), 7.09 (1H, dd, ³J = 5.0 and 3.5 Hz, H^b). ¹³C NMR (CDCl₃): δ 140.9 (quat), 137.7 (quat), 133.0 (C²), 128.3 (C^b), 127.5 (C⁴, C⁶), 126.4 (C^a), 124.6 (C^c), 123.3 (quat). MS (EI): *m/z* 318 (M⁺).

(c) **5-[4-(Dimethylamino)phenyl]-1,3-dibromobenzene**. This compound was prepared similarly, starting from tbb (2.00 g, 6.35 mmol) and [4-(dimethylamino)phenyl]boronic acid (1.15 g, 6.99 mmol) in dimethoxyethane (25 mL). After refluxing for 18 h, the mixture was worked up as above but using potassium carbonate as the drying agent in place of magnesium sulfate. The crude product was purified by column chromatography on silica gel, gradient elution from hexane to 75% hexane/25% diethyl ether (v/v), leading to the required product (*R_f* = 0.6 in 75% hexane/25% ether) as a pale-yellow solid (650 mg, 29%). ¹H NMR (400 MHz, CDCl₃): δ 7.61 (2H, d, ⁴J = 2.0 Hz, H⁴), 7.52 (1H, t, ⁴J = 2.0 Hz, H²), 7.43 (2H, d, ³J = 8.0 Hz, H^b), 6.78 (2H, d, ³J = 8.0 Hz, H^a), 3.01 (6H, s, CH₃). ¹³C NMR (CDCl₃): δ 150.5 (quat), 144.8 (quat), 131.0 (C²), 127.8, 127.7 (C⁴, C^b), 125.9 (quat), 123.1 (quat), 112.5 (C^a), 40.4 (CH₃). MS (EI): *m/z* 355 (M⁺). Among side products eluted at higher polarities (*R_f* = 0.2) was 1-bromo-3,5-bis[4-(dimethylamino)phenyl]benzene. ¹H NMR (400 MHz, CDCl₃): δ 7.63 (1H, t, ⁴J = 1.5 Hz, H⁴), 7.57 (2H, d, ⁴J = 1.5 Hz, H²), 7.51 (2H, d, ³J = 8.5 Hz, H^b), 6.80 (2H, d, ³J = 8.5 Hz, H^a), 3.01 (6H, s, CH₃). ¹³C NMR (CDCl₃): δ 150.2 (quat), 143.5 (quat), 133.2 (quat), 127.8 (C^b), 126.7 (C⁴), 123.1 (C²), 122.9 (quat), 112.6 (C^a), 40.5 (CH₃). Anal. Calcd for C₂₂H₂₃N₂Br: C, 66.84; H, 5.86; N, 7.09. Found: C, 66.76; H, 5.85; N, 7.07.

Ligands Prepared Using Route C. (a) 5-(4-Tolyl)-1,3-di(2-pyridyl)benzene (HL⁷). 1,3-Dibromo-5-(4'-tolyl)benzene (0.60 g, 1.84 mmol), 2-(tri-*n*-butylstannyl)pyridine (1.88 g of 91% purity, equivalent to 4.78 mmol), bis(triphenylphosphine)palladium(II) chloride (0.10 g, 0.15 mmol), and lithium chloride (0.78 g, 18.4 mmol) were placed in an oven-dried Schlenk tube, and toluene (10 mL) was added. The mixture was degassed via five freeze–pump–thaw cycles and then heated at reflux under a nitrogen atmosphere for 36 h. After cooling to room temperature, a saturated aqueous solution of potassium fluoride (10 mL) was added and the mixture stirred for 1.5 h. The highly insoluble residue that formed was filtered off under vacuum and washed with more toluene. The solvent was then removed under reduced pressure and the residue taken up into a mixture of dichloromethane (150 mL) and NaHCO₃ (5% by mass, 100 mL). The layers were separated, and the aqueous layer was then further extracted with dichloromethane (2 × 50 mL). The combined organic layers were washed twice with NaHCO₃ (2 × 100 mL), then dried over anhydrous potassium carbonate, and evaporated to dryness. The product was purified by column chromatography on silica gel, gradient elution from hexane to 60% hexane/40% diethyl ether (v/v), affording the required product (*R_f* = 0.3 in 50% hexane/50% ether) as a colorless solid (350 mg, 59%). ¹H NMR (300 MHz, CDCl₃): δ 8.74 (2H, d, ³J = 4.5 Hz, H⁶),

8.57 (1H, t, $^4J = 1.5$ Hz, H^{2'}), 8.29 (2H, d, $^4J = 1.5$ Hz, H^{4'}), 7.89 (2H, d, $^3J = 7.5$ Hz, H³), 7.79 (2H, td, $^3J = 7.5$ Hz, $^4J = 2.0$ Hz, H⁴), 7.67 (2H, d, $^3J = 8.0$ Hz, H^b), 7.27 (4H, m, H⁵, H^a), 2.41 (3H, s, CH₃). ¹³C NMR (CDCl₃): δ 157.2 (quat), 149.6 (C⁶), 142.2 (quat), 140.3 (quat), 137.9 (quat), 137.3 (quat), 136.7 (C⁴), 129.4 (C⁵), 127.2 (C^b), 126.1 (C^{4'}), 124.2 (C^{2'}), 122.3 (C^a), 120.8 (C³), 21.2 (CH₃). MS (EI): m/z 322 (M⁺). Mp: 187 °C.

(b) 5-(2-Thienyl)-1,3-di(2-pyridyl)benzene (HL⁸). This compound was prepared similarly, starting from 1,3-dibromo-5-(2-thienyl)benzene (0.75 g, 2.36 mmol), 2-(tri-*n*-butylstannyl)pyridine (2.66 g of 85% purity, equivalent to 6.14 mmol), bis(triphenylphosphine)palladium(II) chloride (0.13 g, 0.19 mmol), and lithium chloride (1.00 g, 23.6 mmol) in toluene (10 mL). After refluxing for 48 h, the mixture was worked up as above and purified by column chromatography on silica gel, gradient elution from hexane to 25% hexane/75% diethyl ether (v/v), to give the required product ($R_f = 0.4$ in 75% hexane/25% ether) as a colorless solid (530 mg, 71%). Recrystallization from ethanol enabled the remaining trace impurities to be removed. ¹H NMR (500 MHz, CDCl₃): δ 8.62 (2H, d, $^3J = 5.0$ Hz, H⁶), 8.40 (1H, t, $^4J = 1.5$ Hz, H^{2'}), 8.20 (2H, t, $^4J = 1.5$ Hz, H^{4'}), 7.76 (2H, d, $^3J = 7.5$ Hz, H³), 7.64 (2H, td, $^3J = 7.5$ Hz, $^4J = 2.0$ Hz, H⁴), 7.40 (1H, dd, $^3J = 3.5$ Hz, $^4J = 1.0$ Hz, H^c), 7.24 (1H, dd, $^3J = 5.0$ Hz, $^4J = 1.0$ Hz, H^a), 7.18 (2H, ddd, $^3J = 7.5$ and 5.0 Hz, $^4J = 1.5$ Hz, H⁵), 7.02 (1H, dd, $^3J = 5.0$ and 3.5 Hz, H^b). ¹³C NMR (CDCl₃): δ 156.8 (quat), 149.6 (C⁶), 144.0 (quat), 140.5 (quat), 136.8 (C⁴), 135.4 (quat), 128.0 (C^b), 125.0, 124.9 (C^a, C^{4'}), 124.5 (C^{2'}), 123.8 (C^c), 122.4 (C⁵), 120.8 (C³). MS (EI): m/z 314 (M⁺).

(c) 5-[4-(Dimethylamino)phenyl]-1,3-di(2-pyridyl)benzene (HL⁹). This compound was prepared in a similar way, starting from 1,3-dibromo-5-[4-(dimethylamino)phenyl]benzene (0.60 g, 1.69 mmol), 2-(tri-*n*-butylstannyl)pyridine (2.07 g of 78% purity, equivalent to 4.39 mmol), bis(triphenylphosphine)palladium(II) chloride (0.09 g, 0.14 mmol), and lithium chloride (0.72 g, 17 mmol) in toluene (10 mL). After refluxing for 24 h, the mixture was worked up as described above, and the product was purified by column chromatography on silica gel, gradient elution from hexane to 30% hexane/70% diethyl ether, to give the required product ($R_f = 0.3$ in 75% hexane/25% ether) as a colorless solid (400 mg, 67%). ¹H NMR (400 MHz, CDCl₃): δ 8.76 (2H, d, $^3J = 5.0$ Hz, H⁶), 8.52 (1H, t, $^4J = 1.5$ Hz, H^{2'}), 8.28 (2H, d, $^4J = 1.5$ Hz, H^{4'}), 7.93 (2H, d, $^3J = 8.0$ Hz, H³), 7.82 (2H, td, $^3J = 8.0$ Hz, $^4J = 2.0$ Hz, H⁴), 7.71 (2H, d, $^3J = 8.5$ Hz, H^b), 7.30 (2H, ddd, $^3J = 7.5$ and 5.0 Hz, $^4J = 1.5$ Hz, H⁵), 6.88 (2H, d, $^3J = 8.5$ Hz, H^a), 3.03 (6H, s, CH₃). ¹³C NMR (CDCl₃): δ 157.4 (quat), 150.0 (quat), 149.4 (C⁶), 142.3 (quat), 140.1 (quat), 136.9 (C⁴), 128.0 (C^b), 125.6 (C^{4'}), 123.4 (C^{2'}), 122.3 (C⁵), 121.0 (C³), 112.9 (C^a), 40.7 (CH₃). MS (EI): m/z 351 (M⁺). HRMS (ES⁺): 352.1809 (M + H⁺), calcd for C₂₄H₂₂N₃ (M + H⁺): 352.1808. Anal. Calcd for C₂₄H₂₁N₃: C, 82.02; H, 6.02; N, 11.96. Found: C, 81.77; H, 5.99; N, 11.95.

Platinum(II) Complexes. (a) General Procedure for the Preparation of Platinum Complexes [PtL⁴Cl]–[PtL⁸Cl]. Acetic acid (5 mL) was added to a mixture of the ligand HL^{*n*} (typically 0.15 mmol) and K₂PtCl₄ (1 equiv) in an oven-dried Schlenk tube. The mixture was degassed via three freeze–pump–thaw cycles and then heated at reflux under a nitrogen atmosphere for 3 days, generating a yellow or yellow-orange precipitate. Upon cooling to room temperature, the precipitate was separated off from the yellow solution, washed sequentially with methanol, water, ethanol, and diethyl ether (typically 3 × 5 mL of each), and dried under vacuum. Further purification was required for [PtL⁵Cl]–[PtL⁸Cl] to separate traces of protonated ligand, involving the extraction of the solid into dichloromethane (5 × 5 mL) and subsequent removal of solvent

under reduced pressure; for [PtL⁸Cl], further extraction using acetone was necessary. In the case of [PtL⁶Cl], the product was found to be partially protonated at the pendent pyridyl ring; the nonprotonated compound was obtained by washing the dichloromethane solution of the complex with triethylamine (0.05 mL) followed by water (2 × 15 mL).

(i) [PtL⁴Cl] 2-pyridyl: yellow solid, yield 57% after deprotonation as described above. Data for the *protonated* species [PtL⁴-HCl]⁺ initially formed. ¹H NMR (500 MHz, CDCl₃): δ 9.15 (2H, dd, $^3J = 6.0$ Hz, $^4J = 1.0$ Hz, $^3J(^{195}\text{Pt}) = 36.2$ Hz, H⁶), 8.72 (1H, dd, $^3J = 5.0$ Hz, $^4J = 1.0$ Hz, H⁶-pendent py), 8.51 (2H, s, H^{4'}), 8.32 (2H, d, $^3J = 7.5$ Hz, H³), 8.26 (2H, td, $^3J = 7.5$ Hz, $^4J = 1.5$ Hz, H⁴), 8.23 (1H, d, $^3J = 8.0$ Hz, H³-pendent py), 8.02 (1H, td, $^3J = 8.0$ Hz, $^4J = 1.5$ Hz, H⁴-pendent py), 7.61 (2H, ddd, $^3J = 7.0$ and 6.0 Hz, $^4J = 1.5$ Hz, H⁵), 7.47 (1H, ddd, $^3J = 7.5$ and 5.0 Hz, $^4J = 1.0$ Hz, H⁵-pendent py). Data for the *nonprotonated* final product [PtL⁴Cl]. ¹H NMR (500 MHz, CDCl₃): δ 9.31 (2H, dd, $^3J = 5.5$ Hz, $^4J = 1.0$ Hz, $^3J(^{195}\text{Pt}) = 41.4$ Hz, H⁶), 8.69 (1H, d, $^3J = 5.0$ Hz, H⁶-pendent py), 8.06 (2H, s, H^{4'}), 7.94 (2H, td, $^3J = 7.5$ Hz, $^4J = 1.5$ Hz, H⁴-pendent py), 7.80 (4H, m, overlapping H³, H³-pendent py, H⁴), 7.27 (3H, m, overlapping H⁵, H⁵-pendent py). ¹³C NMR (CDCl₃): δ 167.2, 163.2, 157.7, 152.3, 149.8, 141.4, 139.3, 137.2, 134.8, 123.4 (C⁵-pendent py), 123.1 (C^{4'}), 122.1 (C⁵), 120.2, 119.7. MS (EI⁺): m/z 539.051 [M⁺]; calcd for [C₂₁H₁₄N₃-ClPt], 539.052. Anal. Calcd for C₂₁H₁₄N₃ClPt·H₂O: C, 45.29; H, 2.90; N, 7.55. Found: C, 45.04; H, 2.88; N, 7.15.

(ii) [PtL⁵Cl] Mesityl. Complexation was carried out on a smaller scale (0.07 mmol) in this case, leading to the product as an orange solid in 20% yield. ¹H NMR (200 MHz, CDCl₃): δ 9.12 (2H, d, $^3J = 6.0$ Hz, $^3J(^{195}\text{Pt}) = 20.0$ Hz, H⁶), 7.87 (2H, td, $^3J = 7.5$ Hz, $^4J = 2.0$ Hz, H⁴), 7.58 (2H, d, $^3J = 7.5$ Hz, H⁶), 7.26 (2H, dd, $^3J = 7.5$ Hz, 6.0, H⁵), 7.18 (2H, s, H^{4'}), 6.92 (2H, s, H^a), 2.01 (9H, s, CH₃). Anal. Calcd for C₂₅H₂₁N₂ClPt: C, 51.77; H, 3.65; N, 4.83. Found: C, 51.04; H, 3.85; N, 4.49.

(iii) [PtL⁶Cl] biphenyl: yellow solid in 66% yield. ¹H NMR (500 MHz, CDCl₃): δ 9.35 (2H, dd, $^3J = 6.0$ Hz, $^4J = 2.0$ Hz, $^3J(^{195}\text{Pt}) = 39.0$ Hz, H⁶), 7.96 (2H, td, $^3J = 8.0$ Hz, $^4J = 1.5$ Hz, H⁴), 7.76 (2H, d, $^3J = 8.0$ Hz, H³), 7.71 (4H, m, H^b, H^{4'}), 7.67 (4H, m, H², H^a), 7.49 (2H, t, $^3J = 7.5$ Hz, H^a), 7.39 (1H, t, $^3J = 7.5$ Hz, $^4J = 1.8$ Hz, H^c), 7.29 (2H, ddd, $^3J = 7.3$ and 5.9 Hz, $^4J = 1.5$ Hz, H⁵). ¹³C NMR (CDCl₃): δ 167.3, 152.5, 141.5, 140.7, 140.2, 139.3 (C⁴), 129.1 (C^a), 127.9 (C^c), 127.6, 127.4 (C^b or C^b), 127.2 (C^b or C^b), 123.5 (C⁵), 123.3 (C^a), 199.5 (C³). MS (EI): m/z 614.089 [M⁺]; calcd for [C₂₈H₁₉N₂ClPt], 619.088; 613.09 [M – Cl⁺].

(iv) [PtL⁷Cl] tolyl: orange solid in 56% yield. ¹H NMR (400 MHz, CDCl₃): δ 9.31 (2H, dd, $^3J = 5.5$ Hz, $^4J = 1.0$ Hz, $^3J(^{195}\text{Pt}) = 37.6$ Hz, H⁶), 7.96 (2H, td, $^3J = 8.0$ Hz, $^4J = 1.2$ Hz, H⁴), 7.72 (2H, d, $^3J = 8.0$ Hz, H³), 7.58 (2H, s, H^{4'}), 7.51 (2H, d, $^3J = 8.4$ Hz, H^b), 7.28–7.24 (4H, m, H⁵, H^a), 2.42 (6H, s, CH₃). ¹³C NMR (CDCl₃): δ 168.1 (quat), 152.0 (C⁶), 142.3 (quat), 140.1 (C⁴), 138.3 (quat), 136.4 (quat), 136.1 (quat), 129.4 (C⁵), 127.1 (C^b), 123.2 (C^a), 123.0 (C^{4'}), 119.0 (C³), 20.4 (CH₃). MS (LSIMS): m/z 516 (M⁺ – Cl). Anal. Calcd for C₂₃H₁₇N₂PtCl: C, 50.05; H, 3.10; N, 5.08. Found: C, 49.52; H, 3.13; N, 4.80.

(v) [PtL⁸Cl] thienyl: orange solid in 23% yield. ¹H NMR (400 MHz, CDCl₃): δ 9.14 (2H, d, $^3J = 5.0$ Hz, $J(^{195}\text{Pt}) = 37.6$ Hz, H⁶), 7.84 (2H, t, $^3J = 8.0$ Hz, H⁴), 7.60 (2H, d, $^3J = 8.0$ Hz, H³), 7.43 (2H, s, H^{4'}), 7.20 (2H, m, H^a, H^c), 7.13 (2H, dd, $^3J = 8.0$ and 5.0 Hz, H⁵), 7.00 (1H, m, H^b). ¹³C NMR (CDCl₃): δ 150 (C⁶-py), 144 (quat), 142 (quat), 138 (C⁴-py), 130 (quat), 129 (C⁴-thio), 125 (C⁵-thio), 124 (C⁵-py), 123 (C³-thio), 122 (C⁴ and C⁶), 120 (C³-py). MS (LSIMS): m/z 508 (M⁺ – Cl).

(vi) [PtL⁹Cl] Dimethylamino. This complex was prepared using a different solvent system, as used previously for [PtL²Cl].²⁴ HL⁹ (50 mg, 0.14 mmol) was dissolved in acetonitrile (4 mL) in a Schlenk tube, and K₂PtCl₄ (59 mg, 0.14 mmol) was dissolved in water (2 mL) in a separate Schlenk tube. Both solutions were degassed via three freeze–pump–thaw cycles and placed under nitrogen, and the K₂PtCl₄ solution was then transferred to the ligand solution using a cannula. The mixture was heated at reflux under nitrogen for 3 days. Upon cooling, the orange precipitate that had formed was separated by centrifugation, washed with water (4 × 5 mL), ethanol (4 × 5 mL), and diethyl ether (4 × 5 mL), and finally dried under vacuum (48 mg, 58%). ¹H NMR (400 MHz, CDCl₃): δ 9.31 (2H, dd, ³J = 5.5 Hz, ⁴J = 1.5 Hz, ³J(¹⁹⁵Pt) = 37.6 Hz, H⁶), 7.92 (2H, td, ³J = 8.0 Hz, ⁴J = 1.6 Hz, H⁴), 7.71 (2H, dd, ³J = 8.0 Hz, ⁴J = 1.0 Hz, H³), 7.55 (2H, s, H⁴), 7.51 (2H, d, ³J = 7.0 Hz, H^b), 7.24 (2H, dd, ³J = 7.0 Hz, ⁴J = 1.6 Hz, H⁵), 6.83 (2H, d, ³J = 8.4 Hz, H^a), 3.02 (6H, s, CH₃). ¹³C NMR (CDCl₃): δ 208.1 (C²), 168.4 (quat), 152.0 (C⁶), 142.1 (quat), 140 (C⁴), 128 (C^b), 123 (C⁵), 122.5 (C^a), 120.3 (C³), 113.0 (C³), 40.1 (CH₃). MS (LSIMS): *m/z* 581.1 (M⁺), 545.1 (M – Cl⁺). Anal. Calcd for C₂₄H₂₀N₃PtCl^{1/2}·H₂O: C, 48.86; H, 3.59; N, 7.12. Found: C, 48.92; H, 3.33; N, 6.73.

Electrochemical and Photophysical Measurements. Cyclic voltammetry was carried out using a Princeton Applied Research potentiostat 263, using 1 mM solutions of the complexes in 90% CH₃CN/10% CH₂Cl₂, in the presence of [Bu₄N][BF₄] (0.1 M) as the supporting electrolyte. Solutions were purged with nitrogen gas prior to each scan. A three-electrode system was employed using platinum working, reference, and counter electrodes. The voltammograms were referenced to a ferrocene–ferrocenium couple as the standard (*E*⁰ = 0.42 vs SCE).

Absorption spectra were measured on a Biotek Instruments XL spectrometer, using quartz cuvettes of 1-cm path length. Steady-state luminescence spectra were measured using a Jobin Yvon FluoroMax-2 spectrofluorimeter, fitted with a red-sensitive Hamamatsu R928 photomultiplier tube; the spectra shown are corrected for the wavelength dependence of the detector, and the quoted emission maxima refer to the values after correction. Samples for emission measurements were contained within quartz cuvettes of 1-cm path length modified with the appropriate glassware to allow connection to a high-vacuum line. Degassing was achieved via a minimum of three freeze–pump–thaw cycles while connected to the vacuum manifold; the final vapor pressure at 77 K was <10^{–2} mbar, as monitored using a Pirani gauge. Luminescence quantum yields were determined by the method of continuous dilution, using quinine sulfate in 1 M H₂SO₄ (*φ* = 0.546⁴⁴) as the standard; the estimated uncertainty in *φ* is ±20% or better.

Samples for time-resolved measurements were excited at 355 nm using the third harmonic of a Q-switched Nd:YAG laser. The luminescence was detected with a Hamamatsu R928 photomultiplier tube and recorded using a digital storage oscilloscope, before transfer to a PC for analysis. For each complex, a series of at least six solutions were examined over the concentration range 7.5 ×

10^{–6}–1.5 × 10^{–4} M. Plots of the observed decay rate constants versus concentration were linear, and the quoted lifetime at infinite dilution was obtained from the intercept, as described in the Results and Discussion section. The estimated uncertainty in the quoted lifetimes is ±10% or better. Bimolecular rate constants for quenching by molecular oxygen were determined from the lifetimes in degassed and air-equilibrated solutions, taking the concentration of oxygen in CH₂Cl₂ at 0.21 atm of O₂ to be 2.2 mmol dm^{–3}.⁴⁵

Crystallography. The single-crystal X-ray diffraction experiments were carried out at 120 K, using graphite-monochromated Mo K α radiation (λ = 0.710 73 Å) on Bruker SMART area detector diffractometers, equipped with Cryostream N₂ open-flow cooling devices.⁴⁶ A series of narrow ω scans (0.3°) were performed at several φ settings in such a way as to cover a sphere of data to a maximum resolution between 0.70 and 0.77 Å. Cell parameters were determined and refined using the SMART software,⁴⁷ and raw frame data were integrated using the SAINT program.⁴⁸ All three structures were solved by direct methods and refined by full-matrix least squares on *F*² using SHELXTL software.⁴⁹ Reflection intensities were corrected by numerical integration using SHELXTL software, based on crystal measurements and indexing of the faces.⁴⁹ All non-hydrogen atoms were refined with anisotropic displacement parameters, and the hydrogen atoms were positioned geometrically and refined using a riding model. For the structure of HL⁵, the terminal methyl group was modeled as rotationally disordered with occupancies 60% and 40% for the two components. Crystal data and structure refinement parameters are given in Table S2 of the Supporting Information, and further data are in the accompanying CIF file.

Acknowledgment. We thank the EPSRC for a studentship (D.L.R.), Frontier Scientific Ltd. for key starting materials, and the EPSRC National Mass Spectrometry Service Centre for several mass spectra. We are indebted to Dr. A. Beeby for use of the Nd:YAG laser and Dr. R. Katakly and N. Barooah for assistance with electrochemistry. We are grateful to Dr. J. Weinstein for helpful comments and for stimulating discussions on the photophysics of platinum(II) complexes.

Supporting Information Available: Bond lengths and angles for [PL⁶Cl] and [PL³Cl], crystal data and structure refinement parameters, solvatochromic data for [PL⁴Cl]–[PL⁹Cl], correlations of absorption and emission energies vs oxidation potential, and further data in CIF format. This material is available free of charge via the Internet at <http://pubs.acs.org>.

IC051049E

(45) Murov, S. L.; Carmichael, I.; Hug, G. L. *Handbook of Photochemistry*; Marcel Dekker: New York, 1993.

(46) Cosier, J.; Glazer, A. M. *J. Appl. Crystallogr.* **1986**, *19*, 105.

(47) SMART-NT, *Data Collection Software*, version 5.0; Bruker Analytical X-ray Instruments Inc.: Madison, WI, 1999.

(48) SAINT-NT, *Data Reduction Software*, version 5.0; Bruker Analytical X-ray Instruments Inc.: Madison, WI, 1999.

(49) SHELXTL, version 5.1; Bruker Analytical X-ray Instruments Inc.: Madison, WI, 1999.

(44) Meech, S. R.; Phillips, D. J. *Photochem.* **1983**, *23*, 193.